Global and Planetary Change 71 (2010) 218–231

Contents lists available at ScienceDirect

Global and Planetary Change

journal homepage: www.elsevier.com/locate/gloplacha

# A speleothem record of glacial (25–11.6 kyr BP) rapid climatic changes from northern Iberian Peninsula

Ana Moreno [a,b,*], Heather Stoll [c], Montserrat Jiménez-Sánchez [c], Isabel Cacho [d], Blas Valero-Garcés [b], Emi Ito [a], R. Lawrence Edwards [a]

[a] Department of Geology and Geophysics, University of Minnesota, 310 Pillsbury Drive SE, Minneapolis, MN 55455, USA
[b] Instituto Pirenaico de Ecología-CSIC, Avda. Montañana 1005, 50059 Zaragoza, Spain
[c] Departamento de Geología, Universidad de Oviedo, C/ Arias de Velasco, s/n 33005 Oviedo, Spain
[d] Departament d'Estratigrafia, Paleontologia i Geociències Marines, Universitat de Barcelona, C/Marti i Franquès s/n 28080 Barcelona, Spain

ARTICLE INFO

*Article history:*
Received 19 January 2009
Accepted 5 October 2009
Available online 22 October 2009

*Keywords:*
speleothems
northern Iberian Peninsula
Marine Isotope Stage 2
last deglaciation
stable isotopes
trace elements
rapid climate change

ABSTRACT

Low and high frequency climatic fluctuations in northern Iberian Peninsula during the last glacial maximum (LGM) and deglaciation are documented in a stalagmite using $\delta^{18}O$ and $\delta^{13}C$ and hydrologically sensitive trace metal ratios Mg/Ca and Ba/Ca. U/Th dating indicates speleothem growth commenced at 25 kyr BP (Present = year 1950) and extended to 11.6 kyr BP making this one of few European speleothem growing during the last glacial period. Rapid climatic fluctuations as Heinrich event 2 (H2) and Greenland Interstadial (GI-) 2 are well characterized in this record by more arid and cold conditions and by more humid conditions, respectively. Speleothem growth ceased from 18.2 to 15.4 kyr BP (the so-called Mystery Interval) likely reflecting the driest and potentially coldest conditions of this record, coincident with the 2 kyr duration shutdown of the North Atlantic Meridional Overturning Circulation (MOC). A major gradual increase in humidity and possibly in temperature occurred from 15.5 to 13.5 kyr BP, beginning in the Bølling and culminating in the Allerød period. This gradual humidity change contrasts with more abrupt humidity shifts in the Mediterranean, suggesting a different climate threshold for Mediterranean vs. Atlantic margin precipitation.



## 1. Introduction

The last glacial cycle is characterized by the succession of rapid climatic events defined by an abrupt cooling and a more gradual warming (Dansgaard/Oeschger — D/O — stadials and interstadials, respectively) that were first identified in Greenland ice cores and North Atlantic marine records (Dansgaard et al., 1984; Heinrich, 1988). In the region of Iberian Peninsula, high-resolution and multi-proxy studies of marine sediment sequences have demonstrated that cold intervals detected during the last glacial cycle in the Iberian Margin (Lebreiro et al., 1996; de Abreu et al., 2003; Naughton et al., 2007) and in the Mediterranean Sea (Cacho et al., 1999) are coincident with North Atlantic cold periods. In addition, those events are not only characterized by low sea surface temperatures (SSTs) but also by a sharp increase of aridity in the Iberian Peninsula, indicated by increases in steppe vegetation pollen or enhanced inputs of Saharan dust in the studied marine sediments (Sánchez-Goñi et al., 2000, 2002; Moreno et al., 2002; Combourieu Nebout et al., 2002; Bout-Roumazeilles et al., 2007; Fletcher and Sánchez Goñi, 2008). This relationship between "cold northern events" and "dry southern events" is also true for the rapid climate fluctuations that characterized last deglaciation, such as the Younger Dryas (YD) (Cacho et al., 2001; Fletcher and Sánchez Goñi, 2008). Similar marine records studied in the Gulf of Cadiz (Colmenero-Hidalgo et al., 2004) and the Balearic Islands (Frigola et al., 2008) suggest that this trend extends broadly to the Western Mediterranean and Western African margin (Jullien et al., 2007; Tjallingii et al., 2008; Mulitza et al., 2008) during the last glacial period. In Central Europe this relationship is manifested also in terrestrial records, such as loess sequences (Rousseau et al., 2007) and lake sediments (Wohlfarth et al., 2008). In the Iberian Peninsula, even though the marine response is well documented, terrestrial archives highlighting the connection to high latitude climates during the last glacial period are sparse and include only a few lake records: glacial lakes in the Sanabria region (Muñoz Sobrino et al., 2004), Banyoles Lake (Pérez-Obiol and Julià, 1994; Valero-Garcés et al., 1998) and Portalet peatbog in the Pyrenees (González-Sampériz et al., 2006) and Enol Lake in the Cantabrian Mountains (Moreno et al., in press).

* Corresponding author. Instituto Pirenaico de Ecología-CSIC, Avda. Montañana 1005, 50059 Zaragoza, Spain.
*E-mail addresses:* moren079@umn.edu, amoreno@ipe.csic.es (A. Moreno), hstoll@geol.uniovi.es (H. Stoll), mjimenez@geol.uniovi.es (M. Jiménez-Sánchez), icacho@ub.edu (I. Cacho), blas@ipe.csic.es (B. Valero-Garcés), eito@umn.edu (E. Ito), edwar001@umn.edu (R.L. Edwards).

0921-8181/$ – see front matter © 2009 Elsevier B.V. All rights reserved.
doi:10.1016/j.gloplacha.2009.10.002

One of the main challenges for reconstructing paleoclimate during the last glacial period and deglaciation is the lack of accurate and high-resolution absolute chronologies for correlating abrupt climate changes with those in Greenland ice cores. Chronology in marine sediments is usually hindered by the calibration uncertainties, and sedimentation rates in marine cores are generally lower than in the terrestrial records, thus making difficult any inference about leads and lags between different records. Hence, it is challenging to use marine records to test hypotheses about the mechanisms driving abrupt climate change during the Last Termination or along the last glacial cycle (Moreno et al., 2005). In lake archives, organic remains during glacial and deglaciation periods are scarce and age models lack the necessary accuracy to elucidate the terrestrial responses to important climate changes such as the Heinrich Events. Speleothem records offer a valuable alternative because it is possible to construct independent chronologies with U–Th series (e.g. Dorale et al., 2004). In addition, speleothem samples usually provide high-resolution records during extended periods of time, as long as they grow continuously (White, 2004; Fleitmann et al., 2008). Multi-proxy studies, as those combining stable isotopes with trace element ratios in speleothems, help to narrow the uncertainties associated with the interpretation of stable isotope data alone (Johnson et al., 2006).

Speleothem records in southern Europe covering the end of last glacial cycle and last deglaciation have been described from Southern France (Genty et al., 2003, 2006) and Central Italy (Zanchetta et al., 2007), but up to now there are no speleothem records described from the Iberian Peninsula that cover the last deglaciation interval (see Vesica et al., 2000; Domínguez-Villar et al., 2008; Hodge et al., 2008a,b). Therefore, new records are necessary to (1) identify and characterize the terrestrial response in the northern Iberian Peninsula to abrupt climate change events during the end of the last glacial period and deglaciation and to (2) establish the absolute timing of those events and define leads and lags with respect to Greenland ice cores and nearby marine records.

In this study we present the first data from El Pindal Cave, a coastal cave located close to sea level in the northern Iberian Peninsula where a stalagmite record preserves outstanding paleoclimate information spanning most of Marine Isotopic Stage (MIS) 2 and deglaciation, except the 18.2–15.4 kyr interval when growth was interrupted. This mid-latitude site provides an excellent opportunity to check if the regional relationship between cold North Atlantic events and dry Mediterranean phases during the last glacial cycle and deglaciation also occurred in the Atlantic areas of the Iberian Peninsula.

## 2. Cave setting, climate, and hydrology

Pindal Cave (4°30′W, 43°23′N) is located at the eastern part of the region of Asturias (northern Spain) (Fig. 1). The Cave is 590 m long (314 m open to guided tours), trends east–west and the entrance is 24 m above sea level and at a short distance (<10 m) from the modern sea cliff. The cave is developed in a karstic massif composed of Carboniferous limestone of the Barcaliente Formation which has not been dolomitized. The modern topography of the karstic massif is a marine terrace averaging 60 m above sea level. The cave follows two

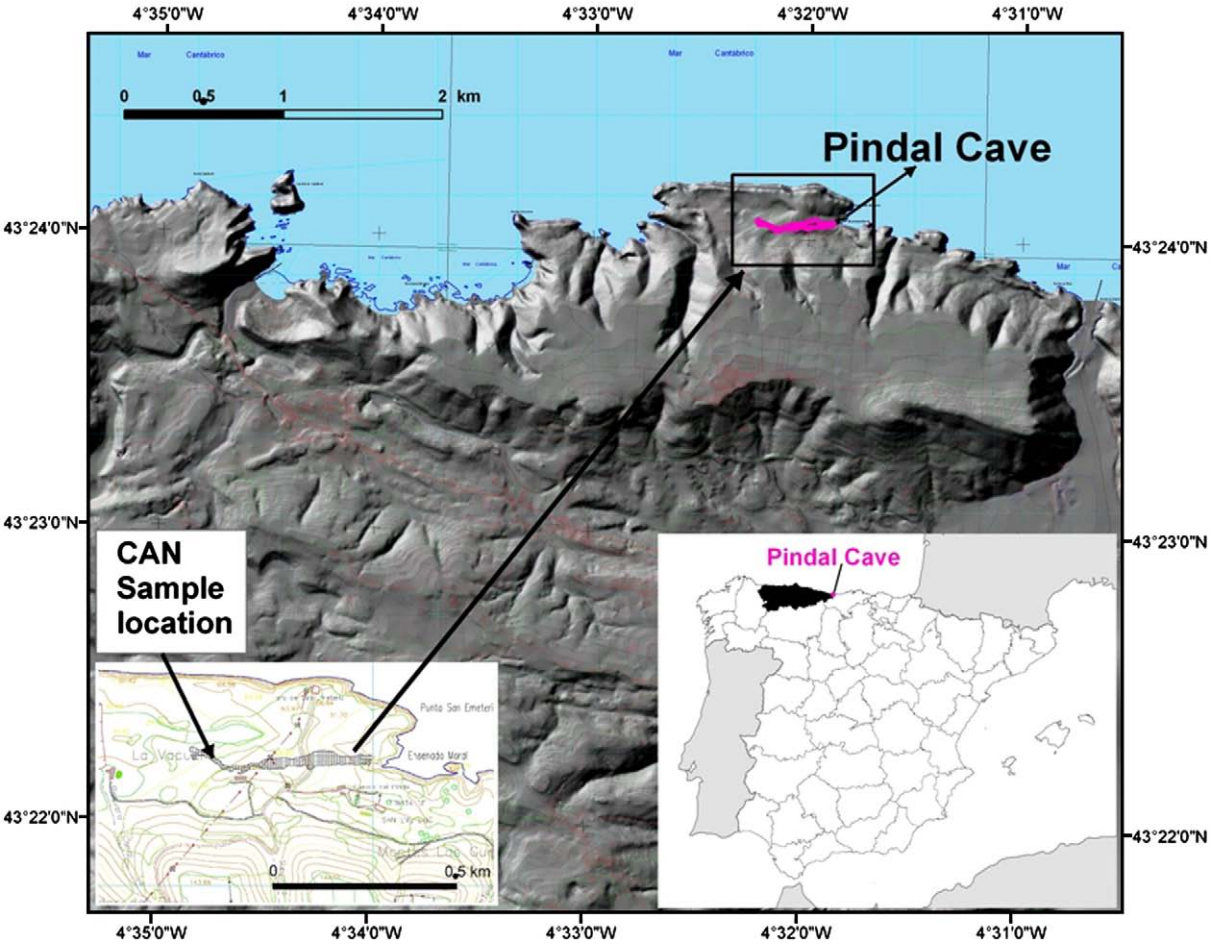


**Fig. 1.** Location of the El Pindal Cave in northern Iberian Peninsula (the region of Asturias is indicated in black). The location of the cave relative to the local topography is also shown. Red line and the hatched area represent the cave in both figures.

sets of subvertical fractures trending E–W (Jiménez-Sánchez et al., 2002). The main cave passage is up to 11 m wide for the first 300 m of the cave, widened by collapse and dissolution of old blocks. The subsequent 300 m of the cave are accessed initially through a narrow (1–3 m) and tall (6 m) vadose incised passage, and subsequently via ascent of a rubble slope from a block collapse into the final wider portion of the cave which maintains its primary phreatic tube architecture. The cave is overlain by limestone ranging from 20 to 60 m thick. The cave is currently well-ventilated and discontinuous measurement of cave $CO_2$ has yielded atmospheric values (390 ppm on average).

The climate in the region has distinct seasons, with higher average precipitation in late fall and early winter and minimum precipitation in the summer months. Average annual rainfall is 1183 mm ± 175 mm, based on 13 yr of instrumental record. Mean cave temperature is 12 °C, close to annual air temperature. Winter months average 9 °C and summer months 20 °C. Modern vegetation above the cave includes pasture and gorse shrub (*Ulex*) subject to occasional burning for pasture regeneration. In some areas overlying the cave, abandonment of agricultural fields in the last century has permitted return of patches of native *Quercus ilex* forest. Soil development is variable depending on overlying vegetation and land use but everywhere soils are rocky and soil depths range from 0 to 60 cm.

Drip rates, monitored for 2 yr at a moderate flow drip location, varied by about 5 fold from maximum values in winter months to minimum drip rates in the summer and occasional 1–2 week periods of no drip (Jiménez-Sánchez et al., 2008c). Higher summer evapotranspiration results in more than two fold reduction in transmissivity of precipitation to drip water (Banasiak, 2008). In winter, there is a variable but typically 1–3 day lag between strong precipitation events and increased drip rates, likely due to the thickness of limestone above the cave and the porosity and permeability of the aquifer. Intense precipitation events in summer do not always result in higher drip rates.

Drip water chemistry at some locations shows a range of Ca concentrations from 60 to 120 ppm positively correlated with drip rate, whereas drip water Ca remains high (110 ppm) at other sites throughout the year (Stoll et al., 2007). In the sites of variable drip water Ca, the range is the same in winter and summer seasons. These data suggest that in the current climate there is approximately constant soil $CO_2$ concentration throughout the year. Assuming seasonal variation in cave $CO_2$ is minor, consistent with our limited data, the hydrochemistry suggests that due to higher winter drip rates speleothem precipitation is currently biased towards the wetter winter season. Minor element chemistry in dripwaters (Banasiak, 2008) shows evidence for both prior calcite precipitation (Huang and Fairchild, 2001), and enrichment in absolute concentrations of Ba and to a lesser extent Mg due to longer residence times in soils as has been observed elsewhere (McDonald et al., 2007). In the modern system, due to the proximity to the coastline and the low Mg content of the host limestone (Mg/Ca = 7 mmol/mol), the majority of Mg in drip waters is derived from marine aerosols. Ba, also low in the host limestone, is derived from soil and dust.

Rainwater $\delta^{18}O$ values above the cave show strong synoptic variation in winter months ranging from −3.0 to −9.0‰ VSMOW (Vienna Standard Mean Ocean Water), with more negative values accompanying more zonal circulation patterns typical of North Atlantic Oscillation (NAO) — climatology. In summer months, due to more locally sourced vapor from warmer ocean temperatures in the western Atlantic, the rainwater $\delta^{18}O$ values rise to −1.0 to −5.0‰ (Jiménez-Sánchez et al., 2008a).

Speleothem deposition in the cave dates from at least 166 kyr BP, the age of the oldest flowstone in the main cave gallery (Jiménez-Sánchez et al., 2006, 2008b). The stalagmite selected for this study, CAN, was recovered from the interior of the cave 500 m from the entrance and grew on a thin (2–5 cm) flowstone crust overlying detrital sand and mud. There had been a local collapse of the flowstone crust on which the stalagmite grew so it was not possible to associate the stalagmite with a particular modern drip system. Most of the stalagmite is composed of typical coalescent columnar fabric crystals, compact and dark beige in color. The intermediate portion of the stalagmite is composed of more porous creamy colored calcite with complex banding structure in the interval 130–150 mm from the base. The sample was entirely composed of calcite, confirmed by petrographic observations and X-ray diffraction analysis. During collection in the cave, the stalagmite broke in half and a 1 cm section 235 mm from the base, was not recovered.

## 3. Material and methods

### 3.1. $^{230}Th$ dating

The speleothem sample was halved along the growth axis, the surface polished and samples for dating were drilled using carbide dental burrs following stratigraphic horizons as in Dorale et al. (2004). Powder amounts ranged from 80 to 270 mg. The chemical procedure used to separate the uranium and thorium is similar to that described in Edwards et al. (1987) and was carried out at the University of Minnesota (USA) laboratories. The calcite powder is dissolved with nitric acid, a mixed $^{229}Th/^{233}U/^{236}U$ tracer is added, and the sample is dried down. After the addition of an iron chloride solution, $NH_4OH$ is added drop by drop until the iron precipitates. The sample is then centrifuged to separate the iron from the rest of the solution and the overlying liquid is removed. After loading the sample into columns containing anion resin, HCl is added to elute the thorium and water is added to elute the uranium. With the uranium and thorium separated, each sample is dried down and dilute nitric acid is added for injection into the ICP-MS.

Analyses were conducted by means of inductively coupled plasma mass spectrometry (ICP-MS) on a Finnigan-MAT Element outfitted with a double focusing sector-field magnet in reversed Nier–Johnson geometry and a single MasCom multiplier from the University of Minnesota laboratories. The instrument was operated at low resolution and in electrostatic peak hopping mode. Further details on instrumental procedures are explained by Shen et al. (2002).

### 3.2. Stable isotopes: $\delta^{18}O$ and $\delta^{13}C$

Each sample was milled using 0.3 or 0.5 mm carbide dental burrs along the length of the speleothem following the growth axes. Spacing between samples ranged from 1 mm (from the base to 230 mm) to 0.5 mm (from 230 mm to the top), with typical powder masses of 80 to 100 μg. Stable isotope ratios of oxygen ($^{18}O/^{16}O$) and carbon ($^{13}C/^{12}C$) were measured for 456 samples. The analyses were performed in two locations: at (1) the Minnesota Isotope Laboratory, Minneapolis, USA and at (2) Scientific-Technical Services (SCT), University of Barcelona, Spain. Both locations use a Finnigan-MAT 252 mass spectrometer, fitted with a Kiel Carbonate Device II in Minnesota and with a Kiel Carbonate Device III in Barcelona. Standards were run every 6 to 10 samples with a reproducibility of 0.02‰ for $\delta^{13}C$ and 0.06‰ for $\delta^{18}O$. Duplicates, run every 10 to 20 samples to check for homogeneity, replicated within 0.1‰ for both oxygen and carbon. Values are reported as $\delta^{18}O$ (‰) and $\delta^{13}C$ (‰) with respect to the Vienna Pee Dee Belemnite (VPDB) standard.

To test for equilibrium calcite precipitation, the correlation between $\delta^{13}C$ and $\delta^{18}O$ values has been evaluated (Fig. 2A). Carbon and oxygen isotopes exhibit a weak but significant correlation during the glacial interval ($r^2 = 0.554$; $p$-value $< 0.01$) while no correlation during the deglaciation interval ($r^2 = 0.032$; $p$-value $< 0.01$) is observed. Additionally, a "Hendy Test" was carried out at 191.5 mm (Fig. 2B) showing low correlation between isotopic ratios along a single layer ($r^2 = 0.004$) and no $\delta^{18}O$ enrichment towards the sides of the stalagmite. Those results suggest that kinetic fractionation has little effect, at least for the interval of the sample where the test was performed, and that the isotopic signals are primarily of climatic origin (Hendy, 1971).

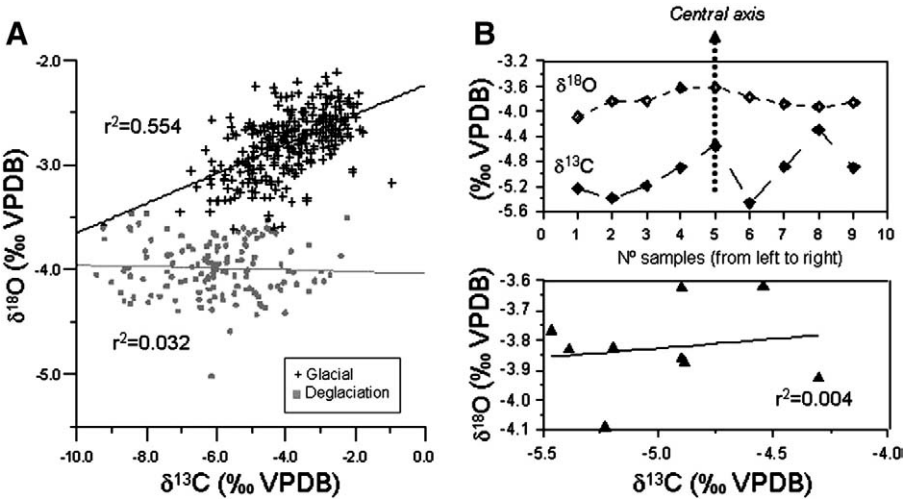


**Fig. 2.** (A) Carbon vs. oxygen isotopes reveal a weak but significant correlation (using Spearman's rank correlation analyses) during the glacial interval (crosses) and no correlation during the deglaciation interval (filled squares). (B) Hendy test: carbon and oxygen isotope composition along a single layer showing spatial distribution and correlation.

### 3.3. Trace element analysis

Elemental chemical composition was analyzed using matrix-matched standards on a simultaneous dual ICP-AES (Thermo ICAP DUO 6300 at University of Oviedo). Samples were drilled using 0.3 or 0.5 mm carbide dental burrs every 1 mm. Drilled powder was placed in tubes cleaned with 10% HCl and rinsed with MilliQ-filtered water. Samples were dissolved in 1.5 mL of 2% $HNO_3$ (Tracepur) immediately prior to analysis and were introduced with a microflow nebulizer (0.2 mL/min) which permitted two replicate analyses. The use of small sample volumes allowed high sample concentrations and detection of a range of trace elements present at low abundances. Samples were run at average Ca concentrations of 200 ppm. Calibration was conducted off-line using the intensity ratio method described by de Villiers et al. (2002). Reported ratios are from measurement of Ca (315.8 nm, in radial mode), from Ba (455.4 nm, in axial mode) and Mg (280.3 nm, in axial mode). The concentration effect, calculated as the relative standard deviation in the Ba/Ca or Mg/Ca ratio for standards diluted over a range from 50–300 ppm Ca, is <2%. Typical Ba concentrations measured in stalagmite are 12 times the nitric acid blank and those of Mg are 338 times the nitric acid blank. A replicate subset of 12 samples (120–156 mm level) dissolved in 0.1 M acetic acid/ammonium acetate buffer revealed no differences in elemental ratios, indicating that there was no differential removal of sorbed components at different dissolution pH ranges.

## 4. Results and interpretation of proxies

### 4.1. Chronology

Fourteen U–Th dates were obtained for CAN, two of which were replicates of CAN-A5 and CAN-A6 drilled from the same holes to obtain more material and reduce errors (Table 1). The uranium concentration is low in this sample ranging from 90 to 500 ppb, thus limiting the accuracy of the dating. Measured $^{230}Th/^{232}Th$ activity ratios indicated that the sample contains little detrital $^{230}Th$ (Table 1). However, a generic bulk earth $^{230}Th/^{232}Th$ ratio ($4.4*10^{-6}\pm2.2*10^{-6}$ atomic ratio) was applied to correct for initial $^{230}Th$. All ages are in stratigraphic order and only some inversions were detected for the lowermost 15 mm of the sample probably related to high $^{232}Th$ content or to alterations of

**Table 1**
$^{230}Th$ dating results from stalagmite CAN from El Pindal Cave, Spain. CAN-A5 and CAN-A6 (in italics) were discarded since two new samples drilled on the same holes (CAN-B2 and CAN-B3, respectively) gave lower errors. Analytical errors are 2$\sigma$ of the mean.

| Sample number | Depth (mm from the base) | $^{238}U$ (ppb) | $^{230}Th/^{238}U$ (activity)[a] | $^{230}Th/^{232}Th$ (activity) | $^{234}U$ (measured)[b] | $^{234}U_{Initial}$ (corrected)[c] | $^{230}Th$ age (uncorrected) (yr BP) | $^{230}Th$ age (corrected)[d] (yr BP) |
|---|---|---|---|---|---|---|---|---|
| CAN-C2 | 15 | 180 ± 0.3 | 0.24142 ± 0.00162 | 163.55 ± 1.35 | 164.9 ± 2.1 | 177.0 ± 2.3 | 25161 ± 195 | 25050 ± 203 |
| CAN-D1 | 32 | 497 ± 1.8 | 0.22819 ± 0.00201 | 193.61 ± 8.05 | 134.8 ± 2.9 | 144.4 ± 3.1 | 24347 ± 249 | 24277 ± 251 |
| CAN-A2 | 60 | 149 ± 0.4 | 0.22207 ± 0.00239 | 160.10 ± 2.40 | 154.2 ± 4.2 | 164.6 ± 4.5 | 23223 ± 293 | 23117 ± 297 |
| CAN-A3 | 80 | 111 ± 0.2 | 0.22783 ± 0.00317 | 15.40 ± 0.21 | 164.2 ± 3.4 | 175.0 ± 3.7 | 23604 ± 373 | 22481 ± 674 |
| CAN-B1 | 120 | 188 ± 0.4 | 0.19285 ± 0.00163 | 221.13 ± 2.44 | 162.2 ± 2.2 | 171.5 ± 2.3 | 19685 ± 186 | 19619 ± 188 |
| CAN-A4 | 175 | 120 ± 0.3 | 0.19079 ± 0.00378 | 143.86 ± 3.70 | 228.2 ± 4.3 | 240.2 ± 4.5 | 18298 ± 399 | 18204 ± 401 |
| CAN-B2 | 180 | 201 ± 0.5 | 0.15603 ± 0.00163 | 77.32 ± 0.87 | 165.7 ± 2.2 | 173.1 ± 2.3 | 15602 ± 178 | 15450 ± 193 |
| *CAN-A5* | *180* | *117 ± 1.4* | *0.14980 ± 0.00276* | *176.71 ± 4.90* | *177.1 ± 35.4* | *184.6 ± 37* | *14781 ± 564* | *14718 ± 563* |
| CAN-1 | 205 | 151 ± 0.5 | 0.13032 ± 0.00169 | 269.36 ± 9.68 | 112.4 ± 5.2 | 116.8 ± 5.4 | 13559 ± 199 | 13521 ± 200 |
| CAN-3 | 215 | 109 ± 0.5 | 0.11937 ± 0.001920 | 770.65 ± 104.17 | 68.2 ± 5.8 | 70.7 ± 6 | 12906 ± 233 | 12894 ± 233 |
| CAN-B3 | 225 | 161 ± 0.3 | 0.12139 ± 0.00162 | 404.24 ± 10.7 | 81.1 ± 2.5 | 84.1 ± 2.6 | 12957 ± 185 | 12933 ± 185 |
| *CAN-A6* | *225* | *105 ± 0.3* | *0.11853 ± 0.00300* | *94.94 ± 2.83* | *81.5 ± 3.9* | *84.5 ± 4.1* | *12628 ± 341* | *12526 ± 345* |
| CAN-C3 | 230 | 165 ± 0.3 | 0.11765 ± 0.00140 | 894.01 ± 58.50 | 78.5 ± 2.1 | 81.3 ± 2.2 | 12567 ± 160 | 12556 ± 160 |
| CAN-A7 | 265 | 91 ± 0.3 | 0.11809 ± 0.00337 | 246.16 ± 15.45 | 159.3 ± 5.8 | 164.6 ± 6 | 11676 ± 356 | 11640 ± 356 |

[a] $[^{230}Th/^{238}U]_{activity} = 1 - e^{-\lambda 230 T} + (\delta^{234}U_{measured}/1000)[\lambda_{230}/(\lambda_{230}-\lambda_{234})](1 - e^{-(\lambda 230 - \lambda 234)T})$, where $T$ is the age. Decay constants are $9.1577\times10^{-6}yr^{-1}$ for $^{230}Th$, $2.8263\times10^{-6}yr^{-1}$ for $^{234}U$, and $1.55125\times10^{-10}yr^{-1}$ for $^{238}U$ (Cheng et al., 2000).

[b] $\delta^{234}U = ([^{234}U/^{238}U]_{activity} - 1)\times1000$.

[c] $\delta^{234}U_{initial}$ corrected was calculated based on $^{230}Th$ age (T), i.e., $\delta^{234}U_{initial} = \delta^{234}U_{measured} \times e^{\lambda 234 * T}$, and $T$ is corrected age.

[d] Age corrections were calculated using an average crustal $^{230}Th/^{232}Th$ atomic ratio of $4.4\times10^{-6}\pm2.2\times10^{-6}$. This is the value for a material at secular equilibrium, assuming a crustal $^{232}Th/^{238}U$ value of 3.8 (Taylor and McLennan, 1995). The errors are arbitrarily assumed to be 50%.

the closed system behaviour, thus leading us to discard that sector of the sample. In this study, we consider the lower 270 mm from the base of the stalagmite, focusing on the last glacial and deglaciation interval. In that interval, one visual discontinuity was clearly detected and, consequently, we dated two subsamples that were taken just above and below the visible hiatus (CAN-A4 and CAN-B2, Table 1). The final age model was constructed by linear interpolation between the available U/Th data (Fig. 3).

The presented record of stalagmite CAN (15 to 270 mm) grew continuously over two intervals (from 25.6 to 18.2 kyr and from 15.4 to 11.6 kyr) with a hiatus in between (Fig. 3). The hiatus corresponds, within the dating error, to the Mystery Interval (Denton et al., 2006). That interval was characterized by low boreal summer and high austral summer insolation, low temperatures in Greenland but sea level rise (Denton et al., 2005). The Mystery Interval includes the Heinrich Event 1 (H1), an event considered very cold and probably dry in this area of the Iberian Peninsula (Naughton et al., 2007). An additional break in deposition occurs at 76 mm in the stalagmite where there is a change in the orientation of the main growth axis and a visible condensed porous horizon although not a significant age difference spanning the break (Fig. 3). This discontinuity in the sample is likely not climatic in origin but reflects tilting of the substrate below the stalagmite.

Growth rate in CAN ranges from 13 to 38 μm/yr, which is relatively low and constant (Fig. 3). Stable isotope and trace element samples, taken with a 0.3 mm or 0.5 mm drill bit, represent 7 to 38 yr depending on the growth rate. The isotope samples were taken every 0.5 mm for the average sampling resolution of 33.4 yr. Trace element samples were taken every 1 mm for the average resolution of 56.5 yr.

### 4.2. The $\delta^{13}C$ record

The overall variation of the $\delta^{13}C$ record is 7.4‰, with a mean value of −4.6‰ (Fig. 4). During Greenland Stadial (GS)-3, the $\delta^{13}C$ values are relatively low with a clear tendency to more negative values towards the end of the interval, reaching the lowest values in GI-2. The transition between GI-2 and GS-2c is abrupt and recorded as sharp increases in both $\delta^{13}C$ and $\delta^{18}O$ isotope values, taking place at 22.8 kyr (Fig. 4). The highest $\delta^{13}C$ values are reached during the LGM (−2.0‰). After the hiatus (18.2–15.4 kyr), $\delta^{13}C$ values decrease gradually and reach the isotopically lowest values during the Allerød period (≈13.5 kyr). Superimposed on this major glacial/interglacial transition is significant high frequency fluctuation of 1–3‰. The $\delta^{13}C$ values increase during the YD to values similar to those of the GS-3.

The carbon isotopic variations may arise from both temperature-driven changes in the intensity of soil microbial activity and humidity-driven changes in the extent of degassing of drip waters. Speleothem $\delta^{13}C$ values can also reflect changes in dominant vegetation types (i.e. the $C_4/C_3$ plant ratio) (Dorale et al., 2002). However $C_4$ plants are not significant around El Pindal today, and pollen records suggest that $C_4$ plants were not any more significant than today during the LGM when tundra vegetation dominated the region (Paquereau, 1980). A more important factor influencing $\delta^{13}C$ variability in our stalagmite may be the plant root respiration and microbial activity of the soil and the epikarst zone. Carbon in speleothem calcite has two main sources: (1) soil $CO_2$ which is controlled by atmospheric $CO_2$, plant respiration, and organic matter degradation; and (2) bedrock carbonate ($CaCO_3$) that is dissolved during seepage. A warmer climate with adequate soil

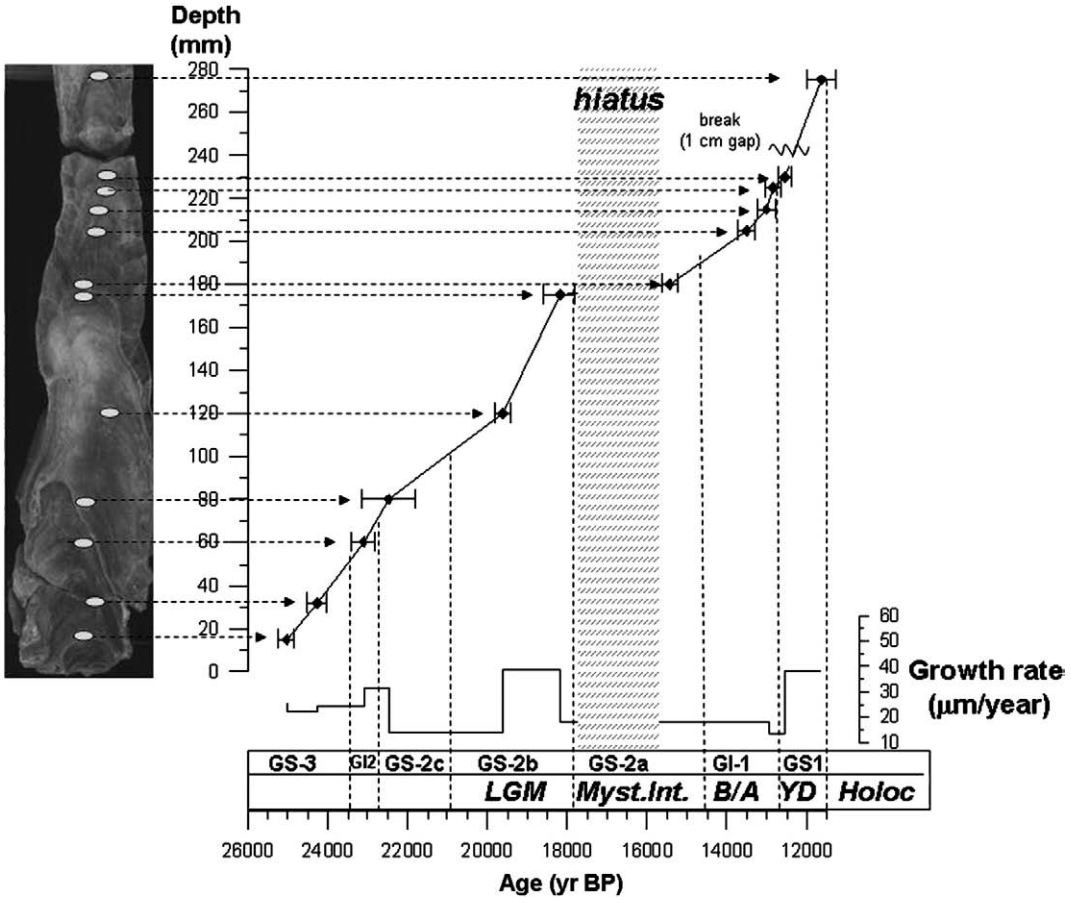


**Fig. 3.** Plot of depth and growth rate vs. age for stalagmite CAN indicating the position of the hiatus. Error bars indicate 2σ error in the dates. A gap of 1 cm resulting for breaking during sample collection is also indicated. Greenland stadials and interstadials are indicated following the chronology and terminology of the INTIMATE group (Lowe et al., 2008). *LGM*: Last Glacial Maximum; *Myst Int:* Mystery Interval; *B/A*: Bølling/Allerød; *YD*: Younger Dryas; *Holoc*: Holocene. The scanned image of CAN is shown with the position of the U–Th drilled samples.

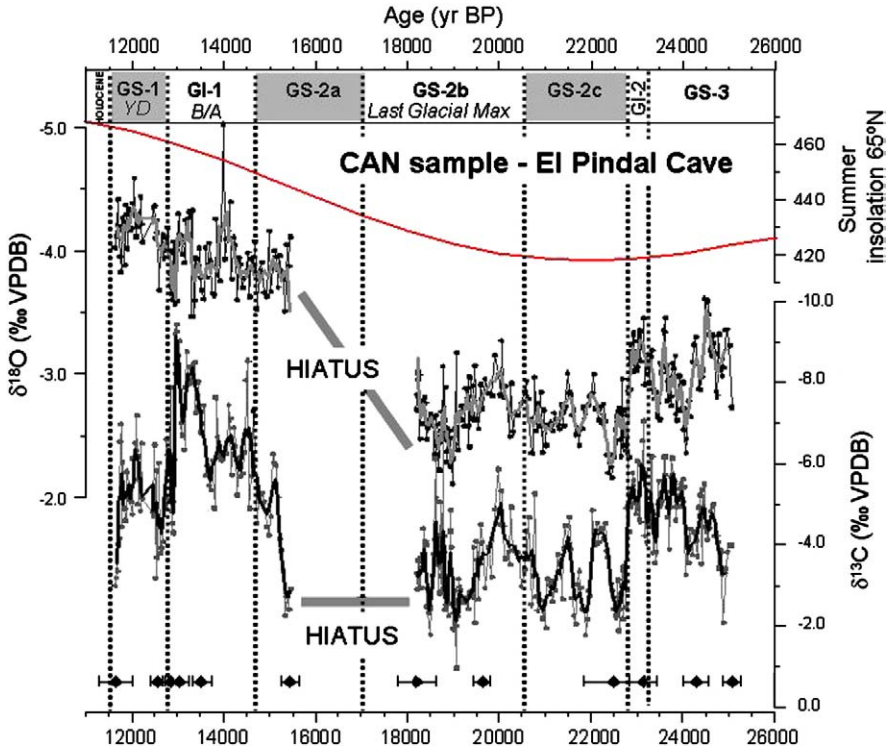


**Fig. 4.** Stalagmite CAN oxygen and carbon isotope values vs. time and average summer insolation for 65°N (red) (Berger and Loutre, 1991). Isotopic records are smoothed with a 5-point moving average (thicker lines). $^{230}$Th ages are also plotted with 2$\sigma$ error bars. Note that isotopes are plotted with reversed $y$-axes.

moisture enhances the microbial activity in the soil above the cave and allows vegetation to develop. That process produces a soil $CO_2$ depleted in $^{13}C$ from respiration and leads to a decrease in the speleothem $\delta^{13}C$ (e.g. Genty et al., 2006). The $\delta^{13}C$ of calcite in the stalagmite is regulated by an additional effect within the cave system, the extent of $CO_2$ degassing prior to stalagmite precipitation. Higher degrees of degassing accompany the slower drip rates and percolation through unsaturated epikarst conduits during periods of lower rainfall and result in differential $^{12}C$ release and more positive $\delta^{13}C$ values in precipitated calcite.

Thus the higher $\delta^{13}C$ mean values of the glacial period likely broadly reflect both colder conditions with reduced soil respiration, as well as more arid conditions with more extensive degassing of drips prior to speleothem precipitation. This latter contribution will be evaluated in subsequent section when $\delta^{13}C$ data are compared with trace elements which are also sensitive to aridity and degassing.

### 4.3. The $\delta^{18}O$ record

The overall variation of the $\delta^{18}O$ record is around 2.5‰, with a mean value of −3.2‰ (Fig. 4). This variation is much smaller than seen in tropical monsoon systems such as southern China or Oman (Fleitmann et al., 2003; Cheng et al., 2006) but comparable to that observed in southern France speleothems (Genty et al., 2006) or in Central Italy (Zanchetta et al., 2007). Similar to the $\delta^{13}C$ record, the highest $\delta^{18}O$ values are reached during the LGM (18.2–22.7 kyr) and GS-2c (Fig. 4). Following the hiatus, the average $\delta^{18}O$ values shift lower by 1.3‰. There is no clear decreasing trend along the Bølling–Allerød (B/A), and the YD is represented by a small negative shift (around 0.2‰).

The results of the Hendy Test (Fig. 2B) suggest that CAN precipitated in isotopic equilibrium. Evaporation of rainwater in the soil or vadose zone is possible but not as important as in semi-arid regions such as Soreq Cave, Israel (Bar-Matthews et al., 1999) due to the positive hydrologic balance in this region. Therefore, we interpret $\delta^{18}O$ record to reflect environmental changes controlled by temperature and the hydrological cycle.

The cave temperature determines the calcite–water fractionation factor so that in equilibrium calcite $\delta^{18}O$ values change by −0.23‰/°C temperature increase (O'Neil et al., 1969). The cave temperature integrates over seasonal variation so the isotopic system records interannual and longer period variation. The new updated global data base of SST for the last glacial maximum indicates that the Bay of Biscay's mean SST was about 6–8 °C (Waelbroeck et al., 2009). High-resolution SST deglaciation reconstructions from the Iberian margin show a pre-B/A warming of about 3 °C between 15.7 and 14.9 kyr BP (Martrat et al., 2007) but possibly as much as 6 °C between the LGM and 14.3 kyr BP (Pailler and Bard, 2002). Such a warming could account for about 0.7 and at most 1.4‰ $\delta^{18}O$ decrease from the LGM to the YD in our record due to the equilibrium temperature fractionation between calcite and drip waters. However, if most of the warming occurred after the end of the Mystery Interval, then cave temperature changes cannot explain much of the mean 1.3‰ shift across the Mystery Interval.

Stalagmite $\delta^{18}O$ values primarily reflect the oxygen isotope composition of rainfall (Dorale et al., 2002). Rainfall $\delta^{18}O$ values are partly set by the $\delta^{18}O$ composition of the ocean source area. Thus, any change in the location of this source area or on the regional oceanography would modify this composition. On glacial–interglacial timescale, one source of low frequency $\delta^{18}O$ variability is the sequestration of isotopically light oxygen in ice sheets. The global oceanic $\delta^{18}O$ increase during the LGM due to the ice sheets was about 1.2‰ (Duplessy et al., 2002), although the change in the North Atlantic may have been slightly less than the global average (Adkins et al., 2002). Only a small portion (<20%) of the ice volume had melted prior to the end of the Mystery Interval, so an insignificant portion of the isotope shift across this boundary could be attributed to ice volume effects. By the end of the YD, sea level rise was about 2/3 complete, so a portion of

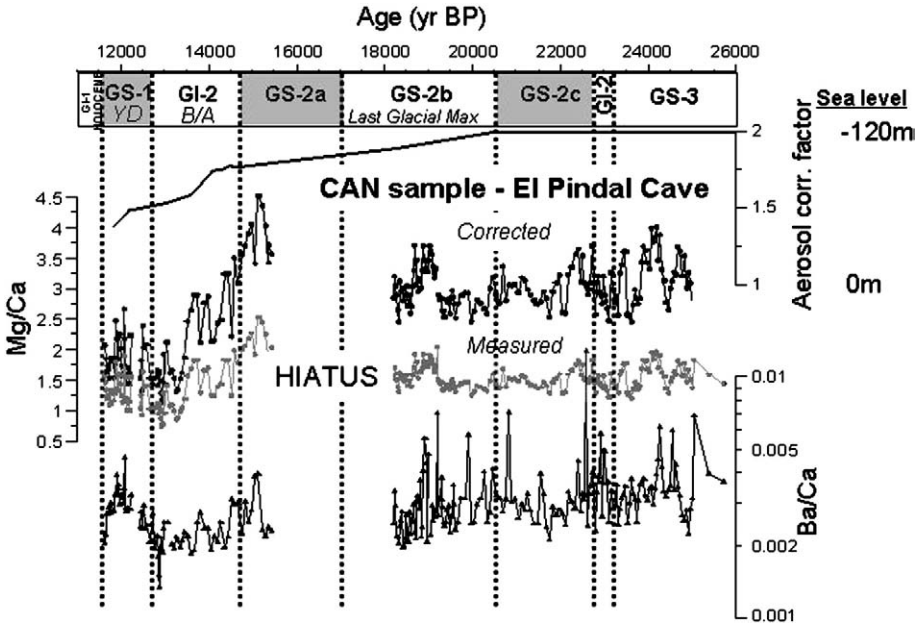


**Fig. 5.** Trace element ratios from CAN stalagmite (Mg/Ca and Ba/Ca). An additional Mg/Ca ratio ("corrected") has been calculated to compensate for reduced Mg supply from sea salt aerosols due to greater distance to the coast during sea level lowstands, as described in the text. The upper panel illustrates the sea level curve used for the correction (data from Stanford et al., 2006, and Peltier and Fairbanks, 2006).

the 0.7‰ isotope shift between the end of the Mystery Interval and YD could be attributed to ice volume effects while a portion could readily be attributed to cave temperature effects.

The main isotopic shift between the LGM and GS-2a appears to require additional processes of fractionation in the hydrological cycle, and such processes may also be important in the higher frequency variability. Today, in low and mid-latitudes, rainfall $\delta^{18}O$ values are controlled by the ratio of transported vapor to local recycled (evaporated) vapor, a ratio well-represented by the P–E (Lee et al., 2007) while local temperatures have a weak effect. In contrast, at higher latitudes the low mean temperatures (<12 °C) induce a higher thermal fractionation decreasing the rainfall $\delta^{18}O$ values between 0.25 and 0.37‰/°C (Lee et al., 2007) and producing the classic relationship exploited by Dansgaard in ice cores (Dansgaard et al., 1984). It is possible that during the glacial period, the opposite fractionation effects of temperature in the hydrological cycle (lower $\delta^{18}O$) and the calcification process (higher $\delta^{18}O$) could have been compensated, cancelling their effect on the speleothem record. This situation could explain why $\delta^{18}O$ values after the hiatus are rather constant while $\delta^{13}C$ values show a larger transition consistent with the deglacial warming observed in SST reconstructions from the Iberian margin. It is also possible that during glacial times changes in seasonality of precipitation toward summer during colder intervals, could have compensated the temperature effect on precipitation $\delta^{18}O$ values, leaving the calcification process as the only fractionation expressed in the speleothem.

The largest 1.3‰ $\delta^{18}O$ shift recognized after the Mystery Interval towards more depleted values is coherent with observed changes in lacustrine carbonates around the Mediterranean region that were attributed to changing moisture source effects and evaporation effects, a pattern contrary to that of lakes from northern and central Europe where $\delta^{18}O$ is more influenced by temperature changes (Roberts et al., 2008). Because of the complexity of these often competing factors (temperature vs. precipitation) on speleothem $\delta^{18}O$ record in this location, it is difficult to obtain unambiguous information from the $\delta^{18}O$ values and thus, like other authors (e.g. Genty et al., 2006) we based most of our interpretations on other geochemical indicators.

### 4.4. Mg/Ca ratios

Measured Mg/Ca ratios range from 0.75 to 2.5 mmol/mol (Fig. 5). They show high frequency, but negligible low frequency variation in the interval from 25–18 kyr, maximum values at 15 kyr just before the B/A, then a steep decline to minimum values in Allerød at 13.2 kyr BP, before increasing slightly during the YD (Fig. 5).

Dripwater Mg/Ca ratios are typically elevated during drier conditions due to the greater degree of prior calcite precipitation from drip waters en route to the stalagmite (Fairchild et al., 2000) and increased contact time between water and soils (e.g. McDonald et al., 2007). These processes are likely the dominant effect on the record, including the high frequency variability and trends during last deglaciation interval. Models of prior calcite precipitation, parameterized with data from modern cave drip waters, indicate that it is possible to attain the observed range of Mg/Ca ratios via a large variation in degree of prior calcite precipitation (Fairchild et al., 2000). The range of prior calcite precipitation required to reproduce the observations diminishes appreciably when we include variations in drip water Mg concentration due to variable soil contact times.

In addition to prior calcite precipitation and soil contact times, the long term trend is likely influenced by an additional factor. In this particular cave setting, drip water Mg is sourced predominantly from marine aerosols (Banasiak, 2008) so changes in aerosol delivery may also affect stalagmite Mg/Ca values. During the LGM, the 120 m sea level drop

**Fig. 6.** A comparison of the CAN record from El Pindal Cave, northern Iberian Peninsula to several records from 26 to 18 kyr. (A) $\delta^{18}O$ (‰ VPDB) and (B) (%) of *N. pachyderma* (sinistra) from MD95-2040 offshore Oporto, Portugal (de Abreu et al., 2003); (C) IRD (grains per gram) and (D) % of semi-arid plants from MD99-2331 offshore Galicia, NW Spain (Naughton et al., 2007); (E) Mg/Ca record, (F) $\delta^{13}C$ and (G) $\delta^{18}O$ (‰ VPDB) profiles from El Pindal cave (this study, note the reversed *y*-axes); (H) NGRIP $\delta^{18}O$ (‰ VSMOW) record from Greenland (Rasmussen et al., 2006) and smoothed with a 5-sample moving average (thicker line) and summer insolation at 65°N. Greenland stadials and interstadials following INTIMATE group (Lowe et al., 2008) and climatic periods are indicated. HE 2 and H2BIS are marked following (Naughton et al., 2007). DO-I 2 refers to Dansgaard–Oeschger interstadial number 2. Arrows indicate correlations among records and tendencies (see text).

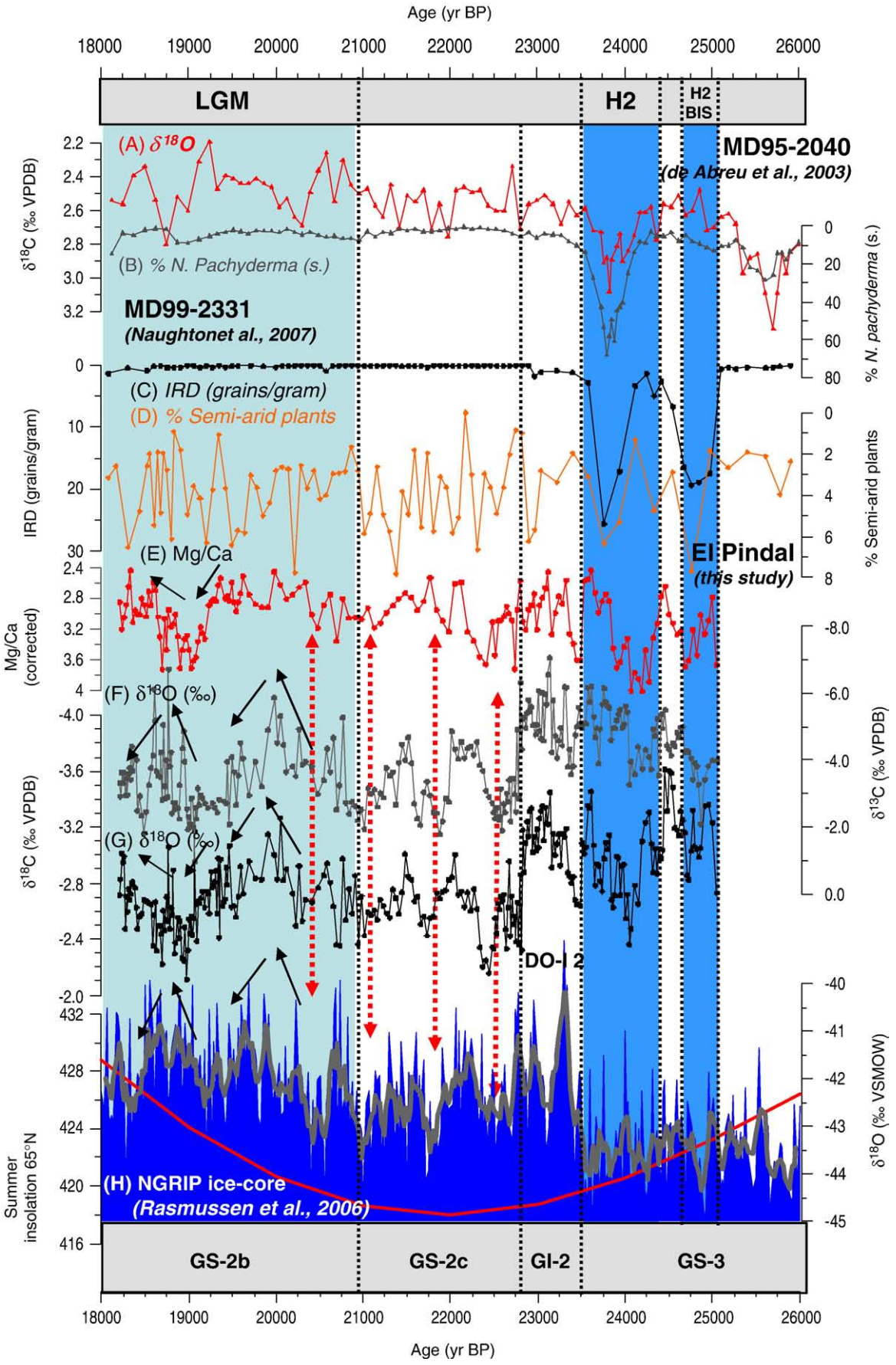

would have increased the distances of the cave to the ocean by some 3–5 km — a distance over which modern drip water sea salt aerosol contributions decrease by 2–3 fold (Banasiak, 2008). Aerosol delivery is expected to increase with sea level rise and proximity to the coast. Aerosol retention would also increase with greater forest cover above the cave which more effectively captures marine aerosols (Appello, 1988), but the pollen analysis indicates that major forest recolonization of this coastal setting did not occur until 9–8 kyr BP (Ramil-Rego et al., 1998). Thus over the time interval studied here, the main modulation of Mg delivery to the cave may be sea level and coastal distance. A simple calculation of the potential influence of changing aerosol Mg is provided in Fig. 5. Mg availability in drip waters is assumed to scale linearly with sea level, with a twofold reduction during glacial times; correcting for this dependency yields an alternative curve for extraction of aridity/humidity trends. Most of the features in this corrected curve are present in the original measurements (Fig. 5). The potential correction would accentuate the dry conditions during the glacial relative to the more humid conditions during the B/A. In fact, the highest values are recorded right after the hiatus which corresponds to the end of the Mystery Interval suggesting that the aridity during this period was even higher than during the LGM. The shift to lower Mg/Ca during the B/A must reflect an increase in the humidity (more rain, higher drip rate and less degassing) since sea level rise, acting alone, would have elevated Mg/Ca ratios.

Mg/Ca ratio variations are highly correlated with $\delta^{13}C$ variations in many parts of the record, particularly 25–23 kyr BP and the 15.4 to 13.2 kyr BP. This correlation suggests either that cold periods of reduced soil microbial activity (higher soil $CO_2$ $\delta^{13}C$) were also very dry (high Mg/Ca), and/or that a significant portion of the $\delta^{13}C$ variation arises from degassing and prior calcite precipitation effects from humidity variations.

### 4.5. Ba/Ca ratios

Ba/Ca ratios range from 0.0013 to 0.0128 mmol/mol and show a similar long term evolution to Mg/Ca. Ba/Ca ratios are high during the glacial interval (25–22 kyr) and at the final part of the Mystery Interval (15.4 kyr), then decrease abruptly by the end of the B/A (Fig. 5). The return to higher Ba/Ca ratios during the YD is particularly pronounced and absolute Ba/Ca ratios are comparable to those of glacial times. In the glacial part of the record high frequency variation has exceptionally large amplitudes (Fig. 5).

As was the case for Mg/Ca, Ba/Ca ratios are expected to be higher during drier periods due to calcite precipitation in soils and water–soil contact times (Ayalon et al., 1999). The latter effect is particularly strong in the modern drip water environment, with Ba showing the largest increase in concentration in drip water of any element during dry periods (Banasiak, 2008). Unlike Mg, Ba has no significant contribution from marine aerosols but is predominantly sourced in soil minerals and dust (Ayalon et al., 1999). Thus the long term trend supports the conclusions derived from corrected Mg/Ca ratios that glacial times were dry and that measured glacial Mg/Ca ratios were depressed by reduced aerosol Mg delivery. The Ba/Ca aridity indicator, not Mg/Ca, provides the clearest definition of the YD period.

## 5. Characterization and timing of major climate transitions in northern Iberian Peninsula and correlation with other records

We discuss the paleoclimate record from the northern Iberian Peninsula in four main stages for the last 25 kyr: (1) from 25 to 22.75 kyr, containing the transition from GS-3 to GI-2; (2) from 22.75 to 18 kyr including the LGM, 3) from 18–15.4 including the Mystery Interval and H1, and (4) from 15.4 to 11.6, covering the B/A and YD events. Many of the climate transitions inferred from isotope and trace element records from CAN stalagmite, including Heinrich and interstadial events, and B/A and YD events are synchronous, within age model uncertainty, to the documented changes in Greenland ice cores (Figs. 6 and 7).

### 5.1. Heinrich events and interstadials from 25 to 22.75 kyr

During the GS-3 and GI-2 intervals, $\delta^{13}C$, $\delta^{18}O$, and Mg/Ca values show a significant coupled variability. Within dating uncertainty it appears that periods of high $\delta^{13}C$, high $\delta^{18}O$, and high Mg/Ca correlate with two pulses of Ice-rafted debris (IRD) in Iberian core MD99-2331 representing H2 (Naughton et al., 2007) (Fig. 6) and two pulses of dust over Greenland (Mayewski et al., 1994). Following H2, Interstadial 2 is well-dated and coincides with low $\delta^{13}C$ and $\delta^{18}O$ values and lower Mg/Ca ratio. Thus, the Mg/Ca record suggests drier conditions in northern Iberia during H2 and more humid conditions during GI-2. Carbon isotopic peaks during H2 may reflect drier conditions and greater degassing of drip waters prior to stalagmite formations, and possibly also colder temperatures with lower rates of soil carbon respiration. The positive oxygen isotope excursion during Heinrich events may reflect greater isotopic fractionation during the formation of calcite in colder temperatures or changes in moisture source or rainfall seasonality (less winter precipitation). Similar to isotope lake records in southern Europe (Roberts et al., 2008), it appears that a classic Dansgaard temperature effect on $\delta^{18}O$ of precipitation is not the dominant feature of the regional hydrological cycle in southern Europe at this timescale.

The CAN record is consistent with arid conditions over a broad region of northern Iberia during H2. In a marine record off the NW corner of the Iberian Peninsula, H2 is characterized by cold SST and an increase of steppe pollen observed as two separated maxima (Naughton et al., 2007) (Fig. 6). Off the Portuguese coast, cold conditions are evident during H2 (de Abreu et al., 2003) although the timing and signal is not exactly the same in two offshore Iberia marine sites, most likely caused by the uncertainty in their age models (Fig. 6). In the Central Pyrenees, the El Portalet lake sequence clearly records H2 event and other cold North Atlantic events during the last deglaciation (H1, Older Dryas, Intra Allerød Cold Period, etc) as cold and dry periods with increases of steppe vegetation and sedimentation of organic–poor, siliciclastic silts (González-Sampériz et al., 2006). In the Cantabrian mountains near the study area, a lake sequence from Lago Enol records an episode of colder and drier conditions that can be related to H2, although the chronology is less precise than for other Iberian sites (Moreno et al., in press). Thus, our speleothem record, due to the high-resolution and precise chronology, is the only terrestrial sequence that up to now supports the evidence from marine pollen records of a two-phase H2.

### 5.2. Climate variability during full glacial conditions

During the GS 2b–c, average values of both $\delta^{13}C$ and $\delta^{18}O$ increased from the previous intervals by 2.5 and 0.8‰ respectively, reaching the highest values of the CAN record. This isotopic enrichment suggests that temperatures were colder during the GS-2c–b than during the previous GS3 and GI2 intervals. Additionally, this section of the stalagmite corresponding to GS 2b–c (90–160 cm) is characterized by a drastic change in the fabric to a porous creamy calcite, contrasting with the coalescent columnar fabric observed for most of the sample. There is no shift in mean Mg/Ca or Ba/Ca ratios indicative of aridity change across this transition, which is coherent with other nearby marine cores also suggesting no changes in aridity (Fig. 6).

The LGM in several Iberian marine and terrestrial records is a cold and relatively dry period although probably not so dry as the Heinrich events because some Pyrenean glaciers seem to have advanced during the LGM (González-Sampériz et al., 2006). In much of Europe, temperatures were too cold or the conditions too dry for stalagmite growth during the LGM. For example, the speleothem from Villars Cave located in Southern France at 175 m above sea level did not grow from 31.5 to 16 kyr, pointing to extremely cold conditions that prevent seepage and calcite precipitation (Genty et al., 2003). In contrast to the CAN isotope record, a gradual warming is observed in Greenland from minimum during GS-3 to slightly warmer

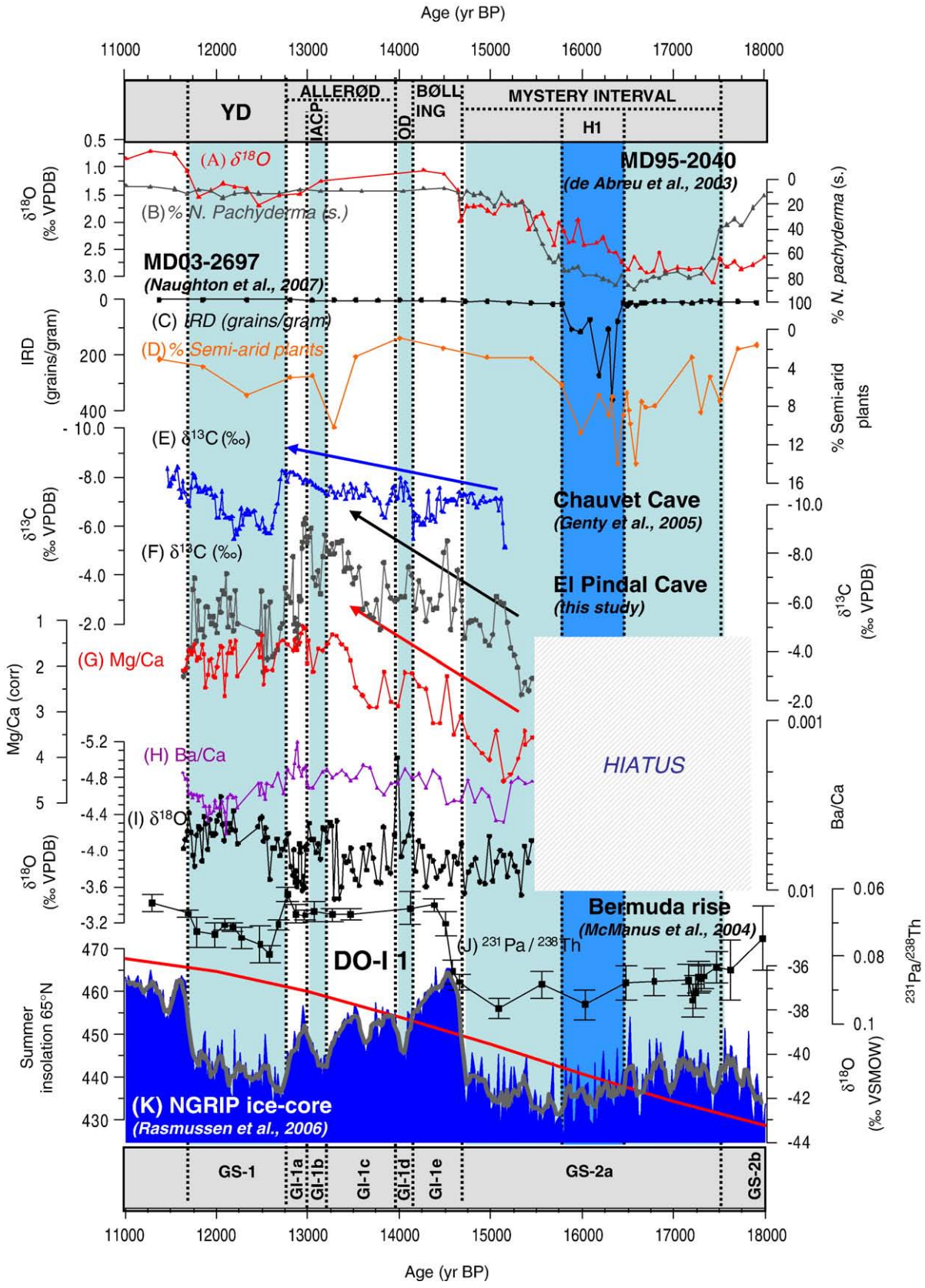


**Fig. 7.** A comparison of the CAN record from El Pindal Cave, northern Iberian Peninsula to several records from 18 to 11 kyr. (A) $\delta^{18}O$ (‰ VPDB) and (B) (%) of *N. pachyderma* (sinistra) from MD95-2040 offshore Oporto, Portugal (de Abreu et al., 2003); (C) IRD (grains per gram) and (D) % of semi-arid plants from MD99-2331 offshore Galicia, NW Spain (Naughton et al., 2007); (E) $\delta^{13}C$ (‰ VPDB)record from Chauvet Cave, Southern France (Genty et al., 2006), (F) $\delta^{13}C$ and (G) $\delta^{18}O$ (‰ VPDB) and (H) Mg/Ca, (I) Ba/Ca profiles from El Pindal cave (this study, note the reversed *y*-axes); (J) $^{231}Pa/^{230}Th$ record from Bermuda rise core GGC5 (McManus et al., 2004); (K) NGRIP $\delta^{18}O$ (‰ VSMOW) record from Greenland (Rasmussen et al., 2006) and smoothed with a 5-point moving average (thicker line), and summer insolation at 65°N. DO-I 1 refers to Dansgaard–Oeschger interstadial number 1. Arrows indicate correlations among records and tendencies (see text).

temperatures at GS-2c and another slight warming during GS-2b (Rasmussen et al., 2006). This variability, although small, is evident in NGRIP, GRIP and GISP2 ice cores (Johnsen et al., 2001).

The environment in northern Iberian Peninsula appears sensitive to high frequency climate variability during this time. There are multi-centennial cycles in $\delta^{18}O$ (amplitude of 0.5‰) and $\delta^{13}C$ (amplitude of 2‰) that are comparable in periodicity to those in Greenland $\delta^{18}O$ (Fig. 6). Unlike the case of the H2 and the GI-2, in this interval the correlation of cycles with Greenland is not precisely established by the U/Th ages (Fig. 3). Linear interpolation between age points suggest that between 23.2 and 20 kyr the high $\delta^{13}C$ and $\delta^{18}O$ values in northern Iberian Peninsula match troughs in $\delta^{18}O$ in Greenland. If the driving mechanisms for isotopic variations during this time are similar to those seen during the earlier fluctuations between H2 and GIS-2, such a correlation is consistent with colder temperatures and dryer climates in northern Iberian Peninsula (higher $\delta^{13}C$ and higher Mg/Ca) coincident with colder temperatures in Greenland (lower $\delta^{18}O$). However, from 19 to 18 kyr (within the LGM), when Greenland $\delta^{18}O$ values were relatively high, the $\delta^{13}C$ record in CAN supports relatively warm temperatures in northern Iberia, but a maximum in $\delta^{18}O$ and a minimum in Mg/Ca suggest rather cold/arid conditions. This apparent inconsistency in the CAN record indicates a more complex relationship for some intervals that remains to be fully understood.

### 5.3. The Mystery Interval

The CAN stalagmite did not grow between 18.2 and 15.4 kyr BP. Although we cannot unequivocally refute changes in the flow routing as an explanation for this growth interruption, several lines of evidence suggest that this hiatus represents conditions which were too cold and/or dry to permit speleothem deposition. First, the resumption of CAN speleothem growth at 15.4 kyr BP appears to reflect a regionally coherent trend of renewed stalagmite growth at other locations in southwestern Europe. In Southern France on the Mediterranean coast at Chauvet cave, the Chauvet 6 stalagmite resumes growth at $15.0 \pm 0.25$ kyr following a hiatus between 24 and 15 kyr BP (Genty et al., 2006). Also in Southern France, near the Atlantic coast, in Villars Cave, the Villars 11 stalagmite begins to grow at $15.2 \pm 0.35$ kyr BP (Genty et al., 2006); older stalagmites in that cave stopped growing at 30 kyr BP suggesting a lapse in speleothem formation between 30 and 15 kyr BP (Genty et al., 2003). Second, in CAN, the first 200–300 yr after the hiatus (from 15.4 to 15.1 kyr BP) are characterized by high values of $\delta^{13}C$, and Mg/Ca and Ba/Ca ratios characteristic of dry conditions and low soil activity in a cold climate, which are likely representative of, but slightly less extreme than, the conditions at this location during the hiatus (Fig. 7).

The hiatus in CAN, considering the dating uncertainty, occurs entirely during the Mystery Interval, defined by Denton et al. (2006) from 17.5 to 14.5 kyr BP. The location of Pindal Cave from which CAN was collected, very near the coast and only 24 m above sea level, appears to be intermediate in sensitivity between other southern European sites (S. France, Italian Alps) where speleothem deposition ceased between 30–25 kyr and 15 kyr BP, and the warmer sites in Tunisia where speleothem growth at La Mine cave is continuous over the last 25 kyr BP (Genty et al., 2006). At CAN, the only major hiatus occurs during the Mystery Interval, suggesting that conditions here during this time period were the most extreme (cold and/or arid) than during any other time in the last 25 kyr.

The Mystery Interval marks the start of the first phase of the last glacial termination. This phase was characterized by the strong reduction of MOC (McManus et al., 2004) relative to levels during the LGM due to high rates of freshwater input during iceberg discharges of H1 (Fig. 7). The shutdown in MOC lasted 2000 yr and caused extremely cold winter temperatures in the North Atlantic area (Denton et al., 2005) and likely formed sea ice, reduced evaporation and consequently, produced a very dry period in Asia (Cheng et al., 2006) and Europe (Allen et al., 1999; Wohlfarth et al., 2008). Because of the close connection between western European temperatures and MOC intensity, temperatures in western Europe would be expected to be colder during the Mystery Interval than during the earlier LGM period. Several other regional records also suggest minimum temperatures during the Mystery Interval rather than the LGM. Marine cores offshore the Iberian Margin indicate colder SST during the Mystery Interval, including H1, than during LGM (de Abreu et al., 2003). In the high elevation (1070 m) Lake Enol record from northern Iberian Peninsula, the lowest sedimentation rates were observed during the Mystery Interval, probably associated with a runoff decrease (Moreno et al., in press). In Lake Estanya located at the Pre-Pyrenees, there is sedimentological and palynological evidence of an H1 more arid than the LGM (Morellón et al., 2009) and similar findings were seen in marine cores from the northwestern margin of the Iberian Peninsula (Naughton et al., 2007) and from the Alborán Sea (Cacho et al., 1999; Fletcher and Sánchez Goñi, 2008). In climate models, H1 was characterized as a colder and drier period than the LGM as well (Kageyama et al., 2005), supporting this interpretation.

### 5.4. The last deglaciation (from 15.4 to 11.6 kyr) including B/A and YD events

The most pronounced climatic change in the entire CAN record occurs between 15.4 and 13.4 kyr BP, as temperature and humidity both rise to the highest values of the record, indicated by the most negative carbon isotopic values (shifting from −2.7 to −9.4‰) and the lowest Mg/Ca and Ba/Ca ratios (Fig. 7). A similar large, gradual $\delta^{13}C$ transition occurs in speleothems from Villars cave, southern France (Genty et al., 2006). In Villars and CAN, the most negative $\delta^{13}C$ values of the last deglaciation are reached during the Allerød period and not during the Bølling period. This timing contrasts with Greenland record where warmer temperatures over Greenland were reached abruptly at the onset of the Bølling period. Other records, such as the Estanya Lake in the Pre-Pyrenees (Morellón et al., 2009), also reached the wettest time of deglaciation during the Allerød. Brief recursions to colder, drier climates in the CAN isotopic record appear to coincide with colder periods in Greenland such as GI-1d and GI-1b, which are correlated to Older Dryas and Intra-Allerød Cold Period, respectively, in European lake records (Watts et al., 1996; von Grafenstein et al., 1999).

The strong regional warming event following the Mystery Interval is coincident with a rapid acceleration of MOC (McManus et al., 2004). Yet, the gradual shift in the CAN and Villars speleothems and pre-Pyrenean lake contrasts with the abrupt shift to warmer temperatures in Greenland at the onset of the Bølling (at $14.69 \pm 0.18$ kyr BP; Lowe et al., 2001). Part of the gradual shift in carbon isotopes in the southern European speleothem records may be due to the longer time required to develop a complex soil and forests after the glacial period. The gradual shift in trace element humidity indicators can be interpreted as suggesting that the climate change itself in the Atlantic sector was more gradual in this region than in Greenland. However, abrupt responses to the Bølling warming and GI-1e are found in other areas of the Mediterranean region. An abrupt drop in speleothem $\delta^{18}O$ values occurs around 16.5 kyr in the Eastern Alps (Frisia et al., 2005), 15.1 kyr BP in Southern France at Chauvet (Genty et al., 2006), and somewhat more gradually between 16 and 15 kyr BP in the Eastern Mediterranean (Bar-Matthews et al., 1999). This pattern suggests strong regional heterogeneity in the rate of deglacial climate change. In addition, the absence of a pronounced change in $\delta^{18}O$ values in Atlantic region speleothems (CAN and Villars) compared to Mediterranean speleothems (Chavet and Soreq caves) suggest different sensitivities of speleothem $\delta^{18}O$ values to climate change (moisture sources, hydrological balances) in these regions. Circum-Mediterranean regions may be more strongly influenced by changes in moisture source and amount effects.

Despite the variation in timing and pace of the deglacial warming and hydrological changes, the abrupt cold interludes such as Older

Dryas and Intra-Allerød Cold Period are synchronous between Greenland and northern Iberian Peninsula CAN site. The Intra-Allerød Cold Period is particularly pronounced (5‰ shift in $\delta^{13}C$; high Mg/Ca and Ba/Ca ratios), even more so than in speleothems from southern France (Fig. 7), and its timing in CAN is well constrained by U-Series dating (Table 1).

The YD event begins notably with intense cooling as interpreted from the abrupt positive shift (3 ‰) in carbon isotopes with a duration of 100 to 200 yr (Fig. 7) and perhaps longer since there is 1-cm gap in recovery of stalagmite following this interval (Fig. 3). This initial shift coincides with the brief reduction in North Atlantic Deepwater formation at the YD onset (Hughen et al., 1998). A positive carbon isotopic shift during the YD was also recognized in a speleothem from La Garma cave from northern Iberian Peninsula (Baldini, 2007). In CAN stalagmite there is a trend towards more arid conditions indicated by Ba/Ca until the end of the YD around 11.6 kyr BP.

## 6. Conclusions

The CAN record, from 25.5 to 11.6 kyr BP documents with high temporal resolution and precise chronology the climate change in northern Iberia during the LGM, and the Late Glacial period through the end of the YD. By combining trace element indicators of aridity with oxygen and carbon isotope tracers sensitive to temperature and moisture source, this record provides an integrated perspective on the climate changes experienced by the region. Carbon isotope variations reflect temperature and humidity regulation of vegetation and soil respiration and drip water degassing. Oxygen isotope variations reflect a more complex array of processes including temperature-driven changes in isotopic fractionation during calcite precipitation and changes in sources of moisture in the hydrological cycle. Once corrected for the influence of aerosol delivery, Mg/Ca, and also Ba/Ca ratios, respond to the hydrological balance (P–E) through soil contact times and extent of prior calcite precipitation.

The CAN speleothem from northern Iberian Peninsula serves as an important link between the millennial climate variability well characterized in the North Atlantic and Greenland, and the correlative abrupt climate changes observed in high accumulation rate marine cores in the western Mediterranean. Furthermore, it appears that this location is particularly sensitive to climate disruptions caused by changes in the North Atlantic MOC. Stalagmite growth ceases only during the 3 kyr shutdown of the MOC known as the Mystery Interval, but not during the preceding glacial maximum or GS-3 stages which are colder in Greenland and periods in which speleothem growth is absent farther north on the Atlantic or Mediterranean coasts of France. Thus, this Mystery Interval is possibly the coldest and driest interval of the whole time span recorded in the speleothem. Cold interludes in the North Atlantic region, such as Heinrich event 2, were characterized by more arid and cold conditions in northern Iberian Peninsula. In contrast, warm GI-2 was characterized by more humid conditions.

The major glacial–interglacial transition is not synchronous among all climate indicators in the stalagmite. Thus, in oxygen isotopes, the main transition occurs during the hiatus between 18.2 and 15.4 kyr BP; values after the hiatus are ~1‰ lower than before. In contrast, the other indicators (Mg/Ca, Ba/Ca and $\delta^{13}C$) suggest that the major shift in humidity between dry glacial conditions and more humid interglacial conditions occurred between 15.4 and 13.4 kyr BP. The increase in humidity is gradual and reaches its peak at 13.4 kyr BP. This gradual change is consistent with that of speleothems from the Atlantic coast of France and lakes in the Pre-Pyrenees, but contrasts with the more abrupt change in temperature in Greenland and in the hydrological cycle in the Mediterranean which occurred at the onset of the Bølling about 14.7 kyr BP. Carbon isotopes and Ba/Ca ratios indicate that the YD represented a return to more arid conditions, particularly during the second half of the interval. Although this site in northern Iberian Peninsula and other sites in the Mediterranean show a generally similar response toward more aridity during cold periods in Greenland, the different temporal rates of response during deglaciation are suggestive of a different climate threshold for Mediterranean vs. Atlantic margin precipitation.

## Acknowledgements

We thank Maria Pumariega, cave supervisor, and the Asturian Ministry of Culture for permission to sample in Pindal Cave. This project was supported by a grant from the Spanish Ministry of Education and Science (CAVECAL: MEC CGL2006-13327-Co4-02 to HMS) and GRACCIE-Consolider (CSD2007-00067). We acknowledge fellowships to A. Moreno from the European Comission's Sixth Framework Program (Marie Curie Fellowship 021673 IBERABRUPT) and from the Spanish Ministry of Science ("Ramón y Cajal" program) and H. Stoll from the Spanish Ministry of Science cofunded by the European Social Fund and an instrumentation grant to H. Stoll from the Asturian Comission of Science and Technology (FICYT) cofinanced by the European Regional Development Funds. We thank M. Prieto for access to laboratory instrumentation at the University of Oviedo and M. Prieto, D. Katsikopoulos for discussion. Joaquín Perona (UB-SCT) and Maniko Solheid (University of Minnesota) are acknowledged for help with the stable isotopes measurements, M. J. Domínguez-Cuesta for her help with Fig. 1 and D. Genty, L. de Abreu and F. Naughton for kindly providing their data.

## References

Adkins, J., McIntyre, K., Schrag, D.P., 2002. The salinity, temperature, and d$^{18}$O of the Glacial Deep Ocean. Science 298, 1769–1773.

Allen, J.R.M., Brandt, U., Brauer, A., Hubberten, H.W., Huntley, B., Keller, J., Kraml, M., Mackensen, A., Mingram, J., Negendank, J.F.W., Nowaczyk, N.R., Oberhänsli, H., Watts, W.A., Wulf, S., Zolitschka, B., 1999. Rapid environmental changes in southern Europe during the last glacial period. Nature 400, 740–743.

Appello, C.A.J., 1988. In: Amsterdam, V.U. (Ed.), Water Quality in Hierdensche Beek Watershed. 100 pp.

Ayalon, A., Bar-Matthews, M., Kaufman, A., 1999. Petrography, strontium, barium and uranium concentrations, and strontium and uranium isotope ratios in speleothems as palaeoclimatic proxies: Soreq Cave, Israel. Holocene 9, 715–722.

Baldini, L.M., 2007. An Investigation of the Controls on the Stable Isotope Signature of Meteoric Precipitation, Cave Seepage Water, and Holocene Stalagmites in Europe. University College Dublin, Dublin, Ireland.

Banasiak, A., 2008. The rain in Spain does not fall mainly on the plain: geochemical variation in cave drip water and stalagmite records from Asturias, northern Spain Undergraduate Senior Honors Thesis, Director Heather M. Stoll, Thesis, Williams College, Williamstown, 110 pp.

Bar-Matthews, M., Ayalon, A., Kaufman, A., Wasserburg, G.J., 1999. The eastern Mediterranean paleoclimate as a reflection of regional events: Soreq cave, Israel. Earth and Planetary Science Letters 166, 85–95.

Berger, A., Loutre, M.F., 1991. Insolation values for the climate of the last 10 million years. Quaternary Science Reviews 10, 297–317.

Bout-Roumazeilles, V., Combourieu Nebout, N., Peyron, O., Cortijo, E., Landais, A., Masson-Delmotte, V., 2007. Connection between South Mediterranean climate and North African atmospheric circulation during the last 50, 000 yr BP North Atlantic cold events. Quaternary Science Reviews 26 (25–28), 3197–3215.

Cacho, I., Grimalt, J.O., Pelejero, C., Canals, M., Sierro, F.J., Flores, J.A., Shackleton, N.J., 1999. Dansgaard-Oeschger and Heinrich event imprints in Alboran Sea temperatures. Paleoceanography 14 (6), 698–705.

Cacho, I., Grimalt, J.O., Canals, M., Sbaffi, L., Shackleton, N.J., Schönfeld, J., Zahn, R., 2001. Variability of the Western Mediterranean sea surface temperatures during the last 25, 000 years and its connection with the northern hemisphere climatic changes. Paleoceanography 16 (1), 40–52.

Cheng, H., Edwards, L.R., Hoff, J., Gallup, C.D., Richards, D.A., Asmerom, Y., 2000. The half-lives of uranium-234 and thorium-230. Chemical Geology 169, 17–33.

Cheng, H., Edwards, R.L., Wang, Y., Kong, X., Ming, Y., Kelly, M.J., Wang, X., Gallup, C.D., 2006. A penultimate glacial monsoon record from Hulu Cave and two-phase glacial terminations. Geology 34 (3), 217–220.

Colmenero-Hidalgo, E., Flores, J.A., Sierro, F.J., Bárcena, M.A., Löwemark, L., Schönfeld, J., Grimalt, J.O., 2004. Ocean surface water response to short-term climate changes revealed by coccolithophores from the Gulf of Cadiz (NE Atlantic) and Alboran Sea (W Mediterranean). Palaeogeography, Palaeoclimatology, Palaeoecology 205, 317–336.

Combourieu Nebout, N., Turon, J.L., Zahn, R., Capotondi, L., Londeix, L., Pahnke, K., 2002. Enhanced aridity and atmospheric high-pressure stability over the western Mediterranean during the North Atlantic cold events of the past 50 k.y. Geology 30 (10), 863–866.

Dansgaard, W., Johnsen, S.J., Clausen, H.B., Dahl-Jensen, D., Gundestrup, N.S., Hammer, C.U., Oeschger, H., 1984. North Atlantic climatic oscillations revealed by deep Greenland ice cores. In: Hansen, J.E., Takahashi, T. (Eds.), Climate Processes and Climate Sensitivity. Maurice Ewing. American Geophysical Union, Washington, pp. 288–298.

de Abreu, L., Shackleton, N.J., Schönfeld, J., Hall, M.A., Chapman, M.R., 2003. Millennial-scale oceanic climate variability off the Western Iberian margin during the last two glacial periods. Marine Geology 196, 1–20.

de Villiers, S., Greaves, M., Elderfield, H., 2002. An intensity ratio calibration method for the accurate determination of Mg/Ca and Sr/Ca of marine carbonates by ICP-AES. Geochemistry Geophysics Geosystems 3.

Denton, G.H., Alley, R.B., Comer, G.C., Broecker, W.S., 2005. The role of seasonality in abrupt climate change. Quaternary Science Reviews 24, 1159–1182.

Denton, G.H., Broecker, W., Alley, R.B., 2006. The mystery interval 17.5 to 14.5 kyr ago. In: Brigham-Grette, J., Kull, C., Kiefer, T. (Eds.), PAGES News, pp. 14–16.

Domínguez-Villar, D., Wang, X., Cheng, H., Martín-Chivelet, J., Edwards, R.L., 2008. A high-resolution late Holocene speleothem record from Kaite Cave, northern Spain: $\delta^{18}O$ variability and possible causes. Quaternary International 187 (1), 40–51.

Dorale, J.A., Edwards, R.L., Onac, B.P., 2002. Stable isotopes as environmental indicators in speleothems. In: Daoxian, Y., Cheng, Z. (Eds.), Karst Processes and the Carbon Cycle. Geological Publishing House, Beijing, China, pp. 107–120.

Dorale, J.A., Edwards, R.L., Alexander, E.C., Shen, C.C., Richards, D.A., Cheng, H., 2004. Uranium-series dating of speleothems: current techniques, limits and applications. In: Mylroie, J.E., Sasowskyr, I.D. (Eds.), Studies of Cave Sediments: Physical and Chemical Records of Paleoclimate. Kluwer Academy/Plenum publishers, New York, pp. 177–197.

Duplessy, J.C., Labeyrie, L., Waelbroeck, C., 2002. Constraints on the ocean oxygen isotopic enrichment between the Last Glacial Maximum and the Holocene: paleoceanographic implications. Quaternary Science Reviews 21, 315–330.

Edwards, R.L., Chen, J.H., Wasserburg, G.J., 1987. 238U–234U–230Th–232Th systematics and the precise measurements of time over the past 500000 years. Earth and Planetary Science Letters 81, 175–192.

Fairchild, I.J., Borsato, A., Tooth, A.F., Frisia, S., Hawkesworth, C.J., Huang, Y.M., McDermott, F., Spiro, B., 2000. Controls on trace element (Sr–Mg) compositions of carbonate cave waters: implications for speleothem climatic records. Chemical Geology 166 (3–4), 255–269.

Fleitmann, D., Burns, S.J., Mudelsee, M., Neff, U., Kramers, J., Mangini, A., Matter, A., 2003. Holocene forcing of the Indian monsoon recorded in a stalagmite from Southern Oman. Science 300 (5626), 1737–1739.

Fleitmann, D., Spötl, C., Newman, L., Kiefer, T. (Eds.), 2008. Advances in Speleothem Research, 16. PAGES news, 40 pp.

Fletcher, W.J., Sánchez Goñi, M.F., 2008. Orbital- and sub-orbital-scale climate impacts on vegetation of the western Mediterranean basin over the last 48, 000 yr. Quaternary Research 70 (3), 451–464.

Frigola, J., Moreno, A., Cacho, I., Canals, M., Sierro, F.J., Flores, J.A., Grimalt, J.O., 2008. Evidence of abrupt changes in Western Mediterranean Deep Water circulation during the last 50 kyr: a high-resolution marine record from the Balearic Sea. Quaternary International 181, 88–104.

Frisia, S., Borsato, A., Spötl, C., Villa, I.M., Cucchi, F., 2005. Climate variability in the SE Alps of Italy over the past 17,000 years reconstructed from a stalagmite record. Boreas 34 (4), 445–455.

Genty, D., Blamart, D., Ouahdi, R., Gilmour, M.A., Baker, A., Jouzel, J., Van-Exter, S., 2003. Precise dating of Dansgaard–Oeschger climate oscillation in western Europe from stalagmite data. Nature 421, 833–837.

Genty, D., Blamart, D., Ghaleb, B., Plagnes, V., Causse, C., Bakalowicz, M., Zouari, K., Chkir, N., Hellstrom, J., Wainer, K., Bourges, F., 2006. Timing and dynamics of the last deglaciation from European and North African $\delta^{13}C$ stalagmite profiles — comparison with Chinese and South Hemisphere stalagmites. Quaternary Science Reviews 25, 2118–2142.

González-Sampériz, P., Valero-Garcés, B.L., Moreno, A., Jalut, G., García-Ruíz, J.M., Martí-Bono, C., Delgado-Huertas, A., Navas, A., Otto, T., J., D.J., 2006. Climate variability in the Spanish Pyrenees during the last 30,000 yr revealed by the El Portalet sequence. Quaternary Research 66, 38–52.

Heinrich, H., 1988. Origin and consequences of cyclic ice rafting in the Northeast Atlantic Ocean during the past 130000 years. Quaternary Research 29, 142–152.

Hendy, C.H., 1971. The isotopic geochemistry of speleothems — I. The calculation of the effects of different modes of formation on the isotopic composition of speleothems and their applicability as palaeoclimatic indicators. Geochimica et Cosmochimica Acta 35 (8), 801–824.

Hodge, E.J., Richards, D.A., Smart, P.L., Andreo, B., Hoffmann, D.L., Mattey, D.P., González-Ramón, A., 2008a. Effective precipitation in southern Spain (266 to 46 kyr) based on a speleothem stable carbon isotope record. Quaternary Research 69 (3), 447–457.

Hodge, E.J., Richards, D.A., Smart, P.L., Ginés, A., Mattey, D.P., 2008b. Sub-millennial climate shifts in the western Mediterranean during the last glacial period recorded in a speleothem from Mallorca, Spain. Journal of Quaternary Science 23 (8), 713–718.

Huang, Y.M., Fairchild, I.J., 2001. Partitioning of $Sr^{2+}$ and $Mg^{2+}$ into calcite under karst-analogue experimental conditions. Geochimica et Cosmochimica Acta 65 (1), 47–62.

Hughen, K.A., Overpeck, J., Lehman, S.J., Kashgarian, M., Southon, J., Peterson, L.C., Alley, R., Sigman, D.M., 1998. Deglacial changes in ocean circulation from an extended radiocarbon calibration. Nature 391, 65–68.

Jiménez-Sánchez, M., Anadon-Ruiz, S., Farias, P., Garcia-Sansegundo, J., Canto-Toimil, N., 2002. Estudio preliminar de la Geomorfología de la Cueva del Pindal (Ribadedeva, Oriente de Asturias). Geogaceta 31, 47–50.

Jiménez-Sánchez, M., Bischoff, J.L., Stoll, H., Aranburu, A., 2006. A geochronological approach for cave evolution in the Cantabrian Coast (Pindal Cave, NW Spain). Annales de Geomorphologie N.F. 147, 129–141.

Jiménez-Sánchez, M., Domínguez-Cuesta, M.J., Banasiak, A., Stoll, H., Vadillo, I., Trigo, R., 2008c. Calibration of cave climate proxies in northern Spain through rainwater and drip water analysis European Geoscience Union General Assembly 2008, Vienna, Austria, p. A-11278.

Jiménez-Sánchez, M., Moreno, A., Stoll, H., Aranburu, A., Uriarte, J., Iriarte, E., Domínguez-Cuesta, M.J., Valero-Garcés, B.L., 2008a. Dataciones cronológicas con U–Th en la Cueva del Pindal (Asturias, N España): implicaciones geomorfológicas. Trabajos de Geomorfología en España 2006–2008, 49–52.

Jiménez-Sánchez, M., Stoll, H.M., Vadillo, I., Lopez-Chicano, M., Dominguez-Cuesta, M., Martin-Rosales, W., Melendez-Asensio, M., 2008b. Groundwater contamination in caves: four case studies in Spain. International Journal of Speleology 37, 53–66.

Johnsen, S.J., Dahl-Jensen, D., Gundestrup, N.S., Steffensen, J.P., Clausen, H.B., Miller, H., Masson-Delmotte, V., Sveinbjörnsdóttir, A.E., White, J., 2001. Oxygen isotope and palaeotemperature records from six Greenland ice-core stations: Camp Century, Dye-3, GRIP, GISP2, Renland and NorthGRIP. Journal of Quaternary Science 16 (4), 299–307.

Johnson, K.R., Hu, C., Belshaw, N.S., Henderson, G.M., 2006. Seasonal trace-element and stable-isotope variations in a Chinese speleothem: the potential for high resolution paleomonsoon reconstruction. Earth and Planetary Science Letters 244, 394–407.

Jullien, E., Grousset, F.E., Malaize, B., Duprat, J., Sánchez-Goñi, M.F., Eynaud, F., Charlier, K., 2007. Low-latitude "dusty events" vs. high-latitude "icy Heinrich events". Quaternary Research 68 (3), 379–386.

Kageyama, M., Combourieu Nebout, N., Sepulchre, P., Peyron, O., Krinner, G., Ramstein, G., Cazet, J.-P., 2005. The Last Glacial Maximum and Heinrich Event 1 in terms of climate and vegetation around the Alboran Sea: a preliminary model-data comparison. Comptes Rendues a l'Acadèmie des Sciences de Paris 337, 983–992.

Lebreiro, S.M., Moreno, J.C., McCave, I.N., Weaver, P.P.E., 1996. Evidence for Heinrich layers off Portugal (Tore Seamount: 39 N, 12 W). Marine Geology 131, 47–56.

Lee, J.E., Fung, I., DePaolo, D.J., Henning, C.C., 2007. Analysis of the global distribution of water isotopes using the NCAR atmospheric general circulation model. Journal of Geophysical Research-Atmospheres 112 (D16).

Lowe, J.J., Hoek, W.Z., group, I., 2001. Inter-regional correlation of palaeoclimatic records for the Last glacial–Interglacial Transition: a protocol for improved precision recommended by the INTIMATE group. Quaternary Science Reviews 20, 1175–1187.

Lowe, J.J., Rasmussen, S.O., Björck, S., Hoek, W.Z., Steffensen, J.P., Walker, M.J.C., Yu, Z.C., 2008. Synchronisation of palaeoenvironmental events in the North Atlantic region during the Last Termination: a revised protocol recommended by the INTIMATE group. Quaternary Science Reviews 27 (1–2), 6–17.

Martrat, B., Grimalt, J.O., Shackleton, N., de Abreu, L., Hutterli, M.A., Stocker, T.F., 2007. Four climate cycles of recurring deep and surface water destabilizations on the Iberian Margin. Science 317, 502–507.

Mayewski, P.A., Meeker, L.D., Whitlow, S., Twickler, M.S., Morrison, M.C., Bloomfield, P., Bond, G., Alley, R.B., Gow, A.J., Grootes, P., Meese, D.A., Ram, M., Taylor, K.C., Wumkes, W., 1994. Changes in atmospheric circulation and ocean ice cover over the North Atlantic during the last 41.000 years. Science 263, 1747–1751.

McDonald, J., Drysdale, R., Hill, D., Chisari, R., Wong, H., 2007. The hydrochemical response of cave drip waters to sub-annual and inter-annual climate variability, Wombeyan Caves, SE Australia. Chemical Geology 244 (3–4), 605–623.

McManus, J., Francois, R., Gherardi, J.M., Keigwin, L., Brown-Leger, S., 2004. Collapse and rapid resumption of Atlantic meridional circulation linked to deglacial climate changes. Nature 428, 834–837.

Morellón, M., Valero-Garcés, B., Vegas, T., González-Sampériz, P., Romero, O., Delgado-Huertas, A., Mata, P., Moreno, A., Rico, M., Corella, J.P., 2009. Late glacial and Holocene palaeohydrology in the western Mediterranean region: the Lake Estanya record (NE Spain). Quaternary Science Reviews 28, 2582–2599.

Moreno, A., Cacho, I., Canals, M., Prins, M.A., Sánchez-Goñi, M.F., Grimalt, J.O., Weltje, G.J., 2002. Saharan dust transport and high latitude glacial climatic variability: the Alboran Sea record. Quaternary Research 58, 318–328.

Moreno, A., Cacho, I., Canals, M., Grimalt, J.O., Sánchez-Goñi, M.F., Shackleton, N.J., Sierro, F.J., 2005. Links between marine and atmospheric processes oscillating at millennial time-scale. A multy-proxy study of the last 50,000 yr from the Alboran Sea (Western Mediterranean Sea). Quaternary Science Reviews 24, 1623–1636.

Moreno, A., Valero-Garcés, B.L., Jiménez Sánchez, M., Domínguez, M.J., Mata, P., Navas, A., González-Sampériz, P., Stoll, H., Farias, P., Morellón, M., Corella, P., Rico, M., in press. The last deglaciation in the Picos de Europa National Park (Cantabrian Mountains, northern Spain). Journal of Quaternary Science. doi:10.1002/jqs.1265.

Mulitza, S., Prange, M., Stuut, J.-B., Zabel, M., von Dobeneck, T., Itambi, A.C., Nizou, J., Schulz, M., Wefer, G., 2008. Sahel megadroughts triggered by glacial slowdowns of Atlantic meridional overturning. Paleoceanography 23 (PA4206). doi:10.1029/2008PA001637.

Muñoz Sobrino, C., Ramil-Rego, P., Gómez-Orellana, L., 2004. Vegetation of the Lago de Sanabria area (NW Iberia) since the end of the Pleistocene: a palaeoecological reconstruction on the basis of two new pollen sequences. Vegetation History and Archaeobotany 13, 1–22.

Naughton, F., Sánchez-Goñi, M.F., Desprat, S., Turon, J.L., Duprat, J., Malaize, B., Joli, C., Cortijo, E., Drago, T., Freitas, M.C., 2007. Present-day and past (last 25000 years) marine pollen signal off western Iberia. Marine Micropaleontology 62, 91–114.

O'Neil, J., Clayton, R., Mayeda, T., 1969. Oxygen isotope fractionation in divalent metal carbonates. Journal of Chemical Physics 30, 5547–5558.

Pailler, D., Bard, E., 2002. High frequency palaeoceanographic changes during the past 140,000 years recorded by the organic matter in sediments of the Iberian margin. Palaeogeography, Palaeoclimatology, Palaeoecology 181, 431–452.

Paquereau, M.M., 1980. Chronologie playnologique du Pleistocene dans le Sud-Ouest de la France. Suplement au Bulletin de l'AFEQ 1, 298–306.

Peltier, W.R., Fairbanks, R.G., 2006. Global glacial ice volume and Last Glacial Maximum duration from an extended Barbados sea level record. Quaternary Science Reviews 25 (23–24), 3322–3337.

Pérez-Obiol, R., Julià, R., 1994. Climate change on the Iberian Peninsula recorded in a 30000 yr pollen record from Lake Banyoles. Quaternary Research 41, 91–98.

Ramil-Rego, P., Rodríguez-Guitián, M., Muñoz-Sobrino, C., 1998. Sclerophyllous vegetation dynamics in the north of the Iberian peninsula during the last 160,00 years. Global Ecology and Biogeography Letters 7, 335–351.

Rasmussen, S.O., Andersen, K.K., Svensson, A., Steffensen, J.P., Vinther, B.M., Clausen, H.B., Siggaard-Andersen, M.L., Johnsen, S.J., Larsen, L.B., Dahl-Jensen, D., Bigler, M., Röthlisberger, R., Fisher, H., Goto-Azuma, K., Hansson, M., Ruth, U., 2006. A new Greenland ice core chronology for the last glacial termination. Journal of Geophysical Research 11 (D06102). doi:10.1029/2005JD006079.

Roberts, N., Jones, M.D., Benkaddour, A., Eastwood, W.J., Filippi, M.L., Frogley, M.R., Lamb, H.F., Leng, M.J., Reed, J.M., Stein, M., Stevens, L., Valero-Garcés, B., Zanchetta, G., 2008. Stable isotope records of Late Quaternary climate and hydrology from Mediterranean lakes: the ISOMED synthesis. Quaternary Science Reviews 27 (25–26), 2426–2441.

Rousseau, D.-D., Sima, A., Antoine, P., Hatté, C., Lang, A., Zöller, L., 2007. Link between European and North Atlantic abrupt climate changes over the last glaciation. Geophysical Research Letters 34 (L22713). doi:10.1029/2007GL031716.

Sánchez-Goñi, M.F., Turon, J.L., Eynaud, F., Gendreau, S., 2000. European climatic response to millenial-scale changes in the atmosphere-ocean system during the Last Glacial period. Quaternary Research 54, 394–403.

Sánchez-Goñi, M.F., Cacho, I., Turon, J.L., Guiot, J., Sierro, F.J., Peypouquet, J.-P., Grimalt, J.O., Shackleton, N.J., 2002. Synchroneity between marine and terrestrial responses to millennial scale climatic variability during the last glacial period in the Mediterranean region. Climate Dynamics 19, 95–105.

Shen, C.C., Edwards, R.L., Cheng, H., Dorale, J.A., Thomas, R.B., Moran, S.B., Weinstein, S.E., Edmonds, H.N., 2002. Uranium and thorium isotopic and concentration measurements by magnetic sector inductively coupled plasma mass spectrometry. Chemical Geology 185, 165–178.

Stanford, J.D., Rohling, E.J., Hunter, S.E., Roberts, A.P., Rasmussen, S.O., Bard, E., McManus, J., Fairbanks, R.G., 2006. Timing of meltwater pulse 1a and climate responses to meltwater injections. Paleoceanography 21 (4), PA4103.

Stoll, H.M., Jimenez-Sanchez, M., Auer, T., Martosdela Torre, E., 2007. Temporal variation in dripwater chemistry in the Cueva de Pindal (Asturias, NW Spain). In: Duran, J.J., Robledo, P.A., Vázquez, J. (Eds.), CUEVAS turísticas: aportación al desarrollo sostenible. Instituto Geológico y Minero de España, Madrid, pp. 191–200. ISBN 84-7840-722-4.

Taylor, S.R., McLennan, S.M., 1995. The geochemical evolution of the continental crust. Reviews of Geophysics 33, 241–265.

Tjallingii, R., Claussen, M., Stuut, J.-B.W., Fohlmeister, J., Jahn, A., Bickert, T., Lamy, F., Rohl, U., 2008. Coherent high- and low-latitude control of the northwest African hydrological balance. Nature Geoscience 1 (10), 670–675.

Valero-Garcés, B.L., Zeroual, E., Kelts, K., 1998. Arid phases in the western Mediterranean region during the last glacial cycle reconstructed from lacustrine records. In: Benito, G., Baker, V.R., Gregory, K.J. (Eds.), Paleohydrology and Environmental Change, pp. 67–80.

Vesica, P.L., Tuccimei, P., Turi, B., Fornós, J.J., Ginés, A., Ginés, J., 2000. Late Pleistocene paleoclimates and sea-level change in the Mediterranean as inferred from stable isotope and U-series studies of overgrowths on speleothems, Mallorca, Spain. Quaternary Science Reviews 19, 865–879.

von Grafenstein, U., Erlenkeuser, H., Brauer, A., Jouzel, J., Johnsen, S.J., 1999. A Mid-European decadal isotope-climate record from 15,500 to 5000 years BP. Science 284, 1654–1657.

Waelbroeck, C., Paul, A., Kucera, M., Rosell-Melé, A., Weinelt, M., Schneider, R., Mix, A.C., Abelmann, A., Armand, L., Bard, E., Barker, S., Barrows, T., Benway, H., Cacho, I., Chen, M.T., Cortijo, E., Crosta, X., de Vernal, A., Dokken, T., Duprat, J., Elderfield, H., Eynaud, F., Gersonde, G., Hayes, A., Henry, M., Hillaire-Marcel, C., Huang, C.C., Jansen, E., Juggins, S., Kallel, N., Kiefer, T., Kienast, M., Labeyrie, L., Leclaire, H., Londeix, L., Mangin, S., Matthiessen, J., Marret, F., Meland, M., Morey, A.E., Mulitza, S., Pflaumann, U., Pisias, N.G., Radi, T., Rochon, A., Rohling, E.J., Sbaffi, L., Schäfer-Neth, C., Solignac, S., Spero, H., Tachikawa, K., Turon, J.L., 2009. Constraints on the magnitude and patterns of ocean cooling at the Last Glacial Maximum. Nature Geosciences 2, 127–132. doi:10.1038/ngeo411.

Watts, W.A., Allen, J.R.M., Huntley, B., Fritz, S.C., 1996. Vegetation history and climate of the last 15,000 years at Laghi di Monticchio, Southern Italy. Quaternary Science Reviews 15, 113–132.

White, W.B., 2004. Paleoclimate records from speleothems in limestone caves. In: Mylroie, J.E., Sasowskyr, I.D. (Eds.), Studies of Cave Sediments: Physical and Chemical Records of Paleoclimate. Kluwer Academy/Plenum Publishers, New York, pp. 135–175.

Wohlfarth, B., Veres, D., Ampel, L., Lacourse, T., Blaauw, M., Preusser, F., Andrieu-Ponel, V., Kéravis, D., Lallier-Vergès, E., Björck, S., Davies, S.M., de Beaulieu, J.-L., Risberg, J., Hormes, A., Kasper, H.U., Possnert, G., Reille, M., Thouveny, N., Zander, A., 2008. Rapid ecosystem response to abrupt climate changes during the last glacial period in western Europe, 40–16 kyr. Geology 36 (5), 407–410.

Zanchetta, G., Drysdale, R.N., Hellstrom, J., Fallick, A.E., Isola, I., Gagan, M.K., Pareschi, M.T., 2007. Enhanced rainfall in the Western Mediterranean during deposition of sapropel S1: stalagmite evidence from Corchia cave (Central Italy). Quaternary Science Reviews 26, 279–286.